THE PHASE BEHAVIOR AND SOLUBILITY RELATIONS OF THE BENZENE-WATER SYSTEM

DISSERTATION

Presented in Partial Fulfillment of the Requirements for the Degree Doctor of Philosophy in the Graduate School of The Ohio State University

By

CHARLES J. REBERT, BChE, MScE.

****

The Ohio State University
1955

Approved by:

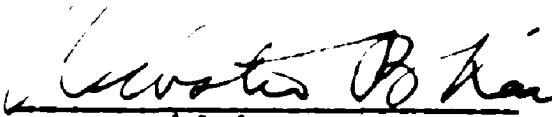

Adviser
Department of Chemical Engineering

ACKNOWLEDGMENTS

I wish to express my gratitude to my advisor, Dr. W. B. Kay, for his patience and assistance in this work and to Dr. J. H. Koffolt for making the entire study program possible.

I wish to acknowledge also the invaluable aid of Dr. J. Bierlein for his fine translation of pertinent parts of Rooseboom's "Heterogeneous Equilibria".

TABLE OF CONTENTS

LIST OF TABLES

LIST OF FIGURES

THE PHASE BEHAVIOR AND SOLUBILITY RELATIONS OF THE BENZENE-WATER SYSTEM

SUMMARY

In order to contribute to the present state of knowledge of the nature of the phase behavior of partially miscible liquid systems, a study of the benzene-water system was undertaken. The pressure at liquid and vapor phase boundaries of fifteen mixtures of benzene and water were determined within the temperature range from 200°C to 357°C. Along with a complete numerical tabulation these data are presented graphically as pressure-temperature, pressure-composition, and temperature-composition phase diagrams to show the nature of the boundaries.

Up to the three-phase critical endpoint the benzene-water system develops in a manner usually ascribed to a partially miscible system in which the vapor composition at a point of univariance lies intermediate to the two liquid compositions. The three-phase critical endpoint occurs at 1364 psia and 268.3°C, and the composition of the critical phase is 25.8 wt.% water while the remaining liquid phase is 92.8 wt.% water.

The pressure, temperature, and composition of the critical solution endpoint are deduced as 2303 psia, 306.4°C, and 59 wt.% water, respectively. At temperatures between these two critical points the phase behavior is

likened to that of the solubility of a dense gas or fluid in a liquid. Definite limiting values of temperature and pressure are assignable to this behavior by extending the three-phase curve up to the critical solution endpoint. This extended curve is not a phase boundary, but the temperature and pressure at a given point represents in a mixture of fixed composition the limit of mutual solubility of the benzene-rich fluid phase and the water-rich liquid phase. At a temperature above or a pressure below the given point the liquid phase begins to vaporize.

Above the critical solution endpoint the vapor-liquid phase boundaries are like those of a normal binary mixture.

INTRODUCTION

The quantitative study of phase behavior has been the subject of experimentation for the past century. The continuing efforts in this field are in themselves indicative of the prominent role played by these studies in the advancement of the physical sciences and of the engineering arts.

Although the concept of the existence of the continuity among phases is generally understood, numerous classifications of types of phase behavior exist for systems which exhibit limited solubility. Thus, there are the classifications of limited mutual solubility of liquids, gas-liquid solubility, and vapor-liquid solubility. Since all of these subjects are examples of phase behavior, the classification may be one of degree rather than fundamentally different types of physical phenomena. The benzene-water system exemplifies all three of the classifications.

The importance of the knowledge of the liquid and gas phase behavior can only be rationalized. The sparing solubility of oil, gas, and water mixtures as we know them at the earth's surface may very well present an entirely different mutual relationship when subject to high underground pressure and temperature. Furthermore, the present technological advancement in the use of high temperature and pressure in chemical industries would be well served by an understanding of the phase relations

particularly in the proposal of mechanisms of chemical reaction rates. High pressure and temperature are emphasized because it is the behavior of partially miscible liquid systems at these conditions where knowledge is lacking.

The behavior of the liquid and gas phases of the benzene-water system throughout most of its saturated temperature range is outlined.

RELATED LITERATURE

The broad basis for the understanding of phase behavior was established by van der Waals just before the turn of the twentieth century. Van der Waals' theory stated simply is that the phase boundaries of liquids and vapors are fixed and continuous curves even though these curves may pass through states which are not physically realizable. These latter states are called metastable and labile states. The mathematical aspect of the theory appears in detail in his book, "Lehrbuches der Thermodynamik" (36).

Van Laar (22) and Kuenen (21) have extended the mathematical treatment of the basic theory into the realm of systems with partially miscible liquids.

The pictorial or graphical appearance of the phase behavior of partially miscible systems is presented by Kuenen (21) and Rooseboom (30). The completion of the latter work due to Buchner, who presented much of the same material in a previous work (4), summarizes for the most part all the studies made on partially miscible systems during that period up to the year 1920.
Ricci (28) has introduced the concept of the miscibility gap as a contribution to the generalization of partially miscible systems. The miscibility gap for a binary system is a volume in space outlined by the dimensions pressure,

temperature, and composition within which the system is unstable and a given phase splits into two mutually saturating phases.

There are apparently no special restrictions on the extent of the miscibility gap for binary systems in general. Likewise, the miscibility gap may occur within any one or all phases. According to Dodge (6) there appears to be a miscibility gap in the highly compressed gas phase of the nitrogen-ammonia system.

The broad scope of the study of the nature of such systems is indicated by the subjects picked at random of work done in this field in recent years. Some of the subjects are as follows: Hildebrand, "Solubility of Water in Hydrocarbons" (11), Tsikilis, "Limited Solubility of the Helium-Ammonia System" (35), Bradbury, "Solubility of Ethylene in Water" (3), Olds, "Dew Point Gas Compositions for the System Water-Methane" (26), Reamer, "Compositions of the Coexisting Phases of n-Butane-Water System in the Three-Phase Region" (27), Schraer, "A Study of the Critical Values of Ethyl Ether Solutions" (33), Ipatieff, "Determination of Critical Temperatures by the Rotary Bomb" (13), Keevil, "Vapor Pressure of Aqueous Solutions at High Temperature" (20), Atack and Schneider, "Solubility Measurements in the Critical Temperature Region" (1), Herington, "Treatment of Binary and Ternary Vapor-Liquid Equilibrium Data on

Systems with More Than One Liquid Phase" (10), Katz and Kobayashi, "Vapor-Liquid Equilibria for Binary Hydrocarbon-Water Systems" (16), and Leland, Jr., McKetta, Jr., and Kobe, "Phase Equilibrium in the 1-Butene-Water System" (24).

The Classic Identification of Partially Miscible Systems

For binary systems where the miscibility gap includes a part or all of the space in the P-T-x solid normally occupied by vapor-liquid transition surfaces, a series of four different cases of isotherms can be evolved (Fig. 1). In the first three cases the sequence of phases at the three-phase pressure is V L_1 L_2, but in the fourth case the sequence is L_1 V L_2. Cases II and III are differentiated from Case I in that they exhibit maximum and minimum boiling points respectively in their miscible regions.

Buchner (4) has developed the space diagram for Case I which is typical of such systems as ethanol-ethane, propanol-ethane, etc. The diagram although supported by some data, is developed largely on theoretical considerations. It does illustrate how the projection of the compositions of the three-phases under their own vapor pressure into the temperature-composition plane (T-x plane) similarly classified partially miscible systems. The projections for Cases I and IV (Fig. 2) are presented by

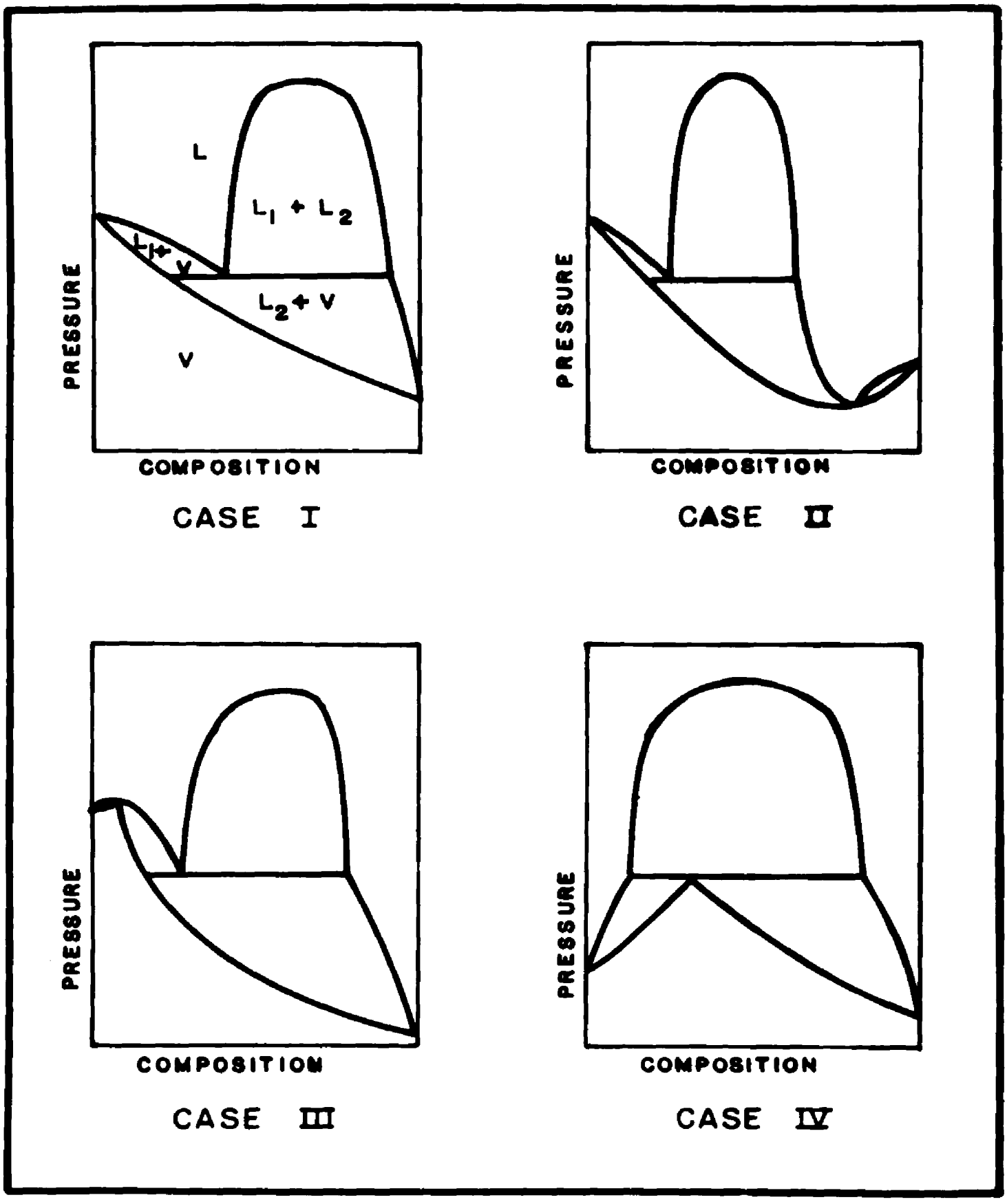

Fig. 1. Characteristic Isotherms of Partially Miscible Binary Systems

Kuenen (21) for the systems ethane-propanol and ether-water, respectively.

One more type of graphical representation of this kind of phase behavior is of interest. Shown in Figure 3 are the curves representing the critical states in the pressure-temperature plane (P-T plane) of all compositions for Cases I and IV. Both diagrams have been derived by the extension of the theory of van der Waals by Rooseboom (30). The points K_1 and K_2 are the vaporization critical values of thepure components. K_3, the three-phase vaporization critical, is observed when one of the liquids and the vapor become a single fluid phase and display the usual optical properties associated with a critical point. The curve K_1K_3 is the locus of the vaporization critical points of mixtures rich in one liquid which are completely miscible. Correspondingly, a portion of the K_2M curve is the locus of vaporization critical points for completely miscible liquid mixtures rich in the second liquid. The remainder of the curve K_2MN is the locus of critical solution points. Points such as S_1 and S_2 at a constant pressure represent the lower and upper critical solution temperatures. The classic example of this phenomena is shown in the nicotine-water system. The dashed curve NK_3 is the three-phase curve and its terminal points are called by Kuenen "the critical end-points".

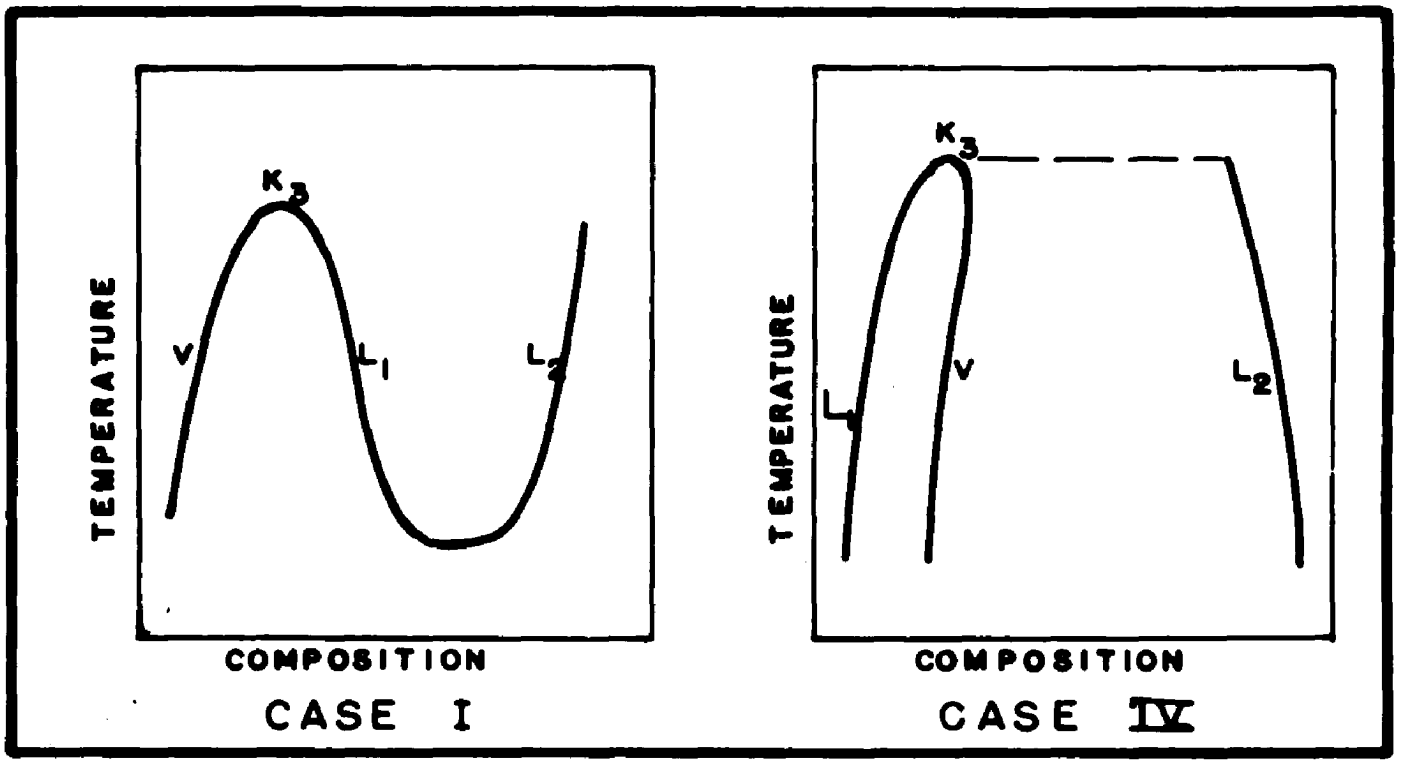

Fig. 2. Projection of the Three-Phase Curve into the T-x Plane of Theoretical Systems

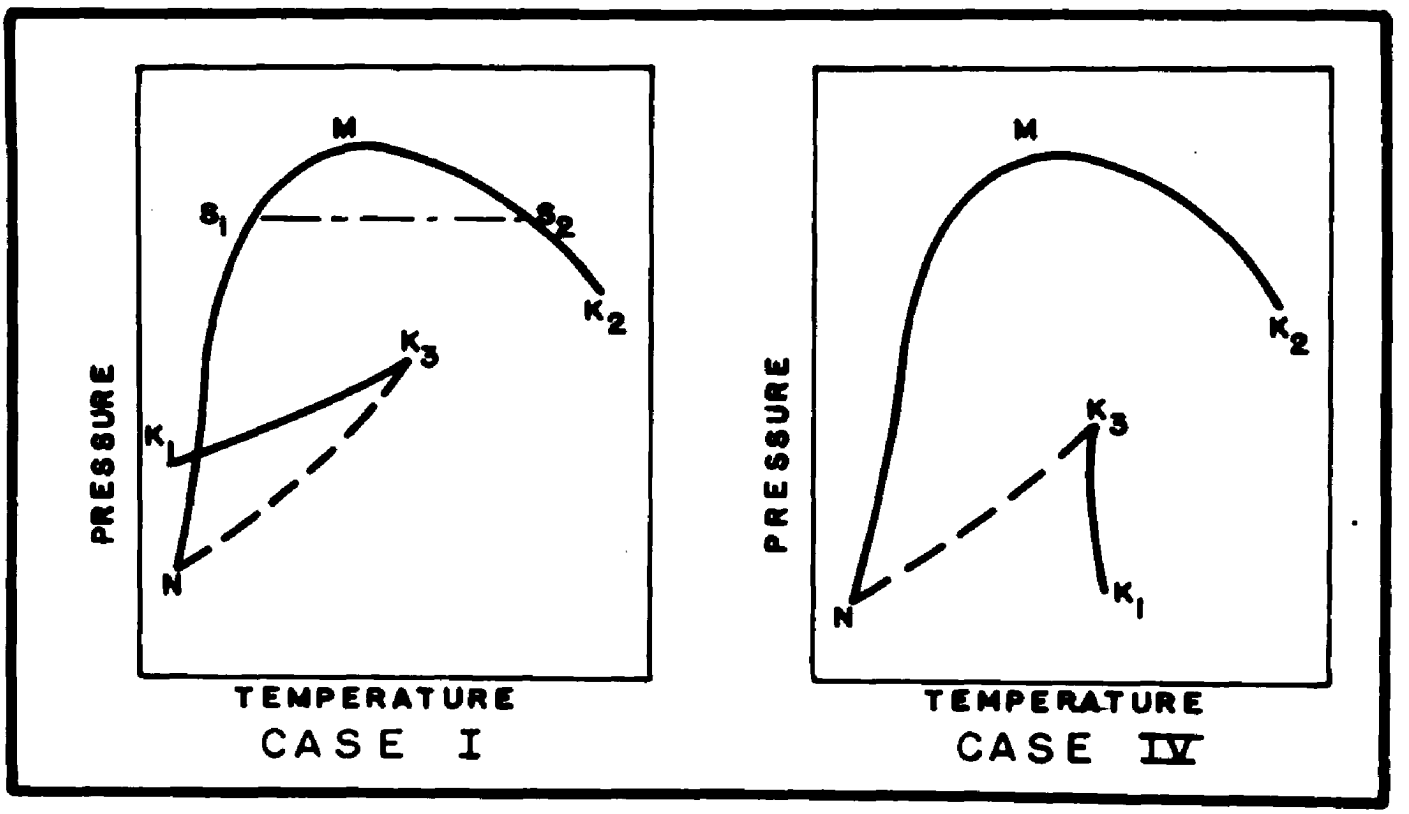

Fig. 3. Locus of Critical States of Theoretical Systems

The Benzene-Water System

According to the classic theory the benzene-water system is identified as Case IV. No system of this case has been investigated quantitatively over its entire range in temperature, pressure, and composition of liquid and vapor phase behavior. Scheffer (31) (32) has measured the temperature and pressure of the three-phase curves up to their vaporization criticals for the systems benzene-water and hexane-water.

For the hexane-water system a number of compositions were taken to determine the effect of temperature and pressure on the solubility of water in hexane rich mixtures. However, the corresponding equilibrium vapor compositions, i.e., heterogeneous azeotropic compositions, and water rich liquid solubilities were not determined. Hence the curves NK_3 and K_1K_3 of Figure 3 are the extent to which quantitative data are available in outlining a Case IV partially miscible liquid system.

The values determined by Scheffer (32) for the benzene-water system are given in Table I, which also summarizes a number of pertinent values of the phase behavior of this system as obtained from the literature.

TABLE I: Summary of the Data from the Literature of the Benzene-Water System

Three-Phase Vapor Pressure (Ref. 32)

T °C	P atm
150	10.6
160	13.2
170	16.4
180	20.1
190	24.6
200	29.8
210	35.9
220	42.9
230	50.9
240.1	60.4
250.2	70.7
260.1	82.2
267.8	92.7

Solubility water in benzene

T °C	Composition	Ref.
5.5	(freezing pt.)	(29)
3	0.030 wt%	(9)
23	0.061	"
40	0.114	"
55	0.184	"
66	0.255	"
77	0.337	"
10	0.03 gm/100 gm	(15)
20	0.044	"
26	0.054	"

Solubility benzene in water

T °C	Composition	Ref.
25	1.79 gm/l	(31)
10	0.153 gm/100 gm	(34)
20	0.175	"
40	0.206	"
60	0.250	"
80	0.325	"
107.4	0.507	"
100	0.2 cc/100 cc	(14)
150	0.6	"
200	2.1	"
250	7.3	"
285	10.6	"
300	14.6	"

Critical Solution Temperature >300°C (8).

Azeotropic composition @ 1 atm 8.89 wt% water (23).

APPARATUS AND PROCEDURE

General

The equipment and procedure used in this investigation were basically those developed by Young (37) and Kay (17). The method consists of confining a known mass of sample of a definite composition over mercury in a capillary tube. The sample in the tube is thermostated and a known pressure is applied. The liquid and vapor phase changes can be observed directly through the tube walls as the pressure is changed. A measurement is made at a point along a phase boundary such as a dew point or bubble point when the sample has attained equilibrium.

Experimental Tube and Compressor Block

The most essential part of the apparatus is the experimental tube, which is the container for the sample. The tubes used in this investigation were made of fused silica with dimensions approximately those shown in Figure 4. The tube was constructed with a thickened collar (A) to fit the mounting assembly in the compressor block, and also fitted with a male tapered joint (B) for mounting on the sample loading apparatus.

The compressor block was a mild steel cylinder machined with a well and internal shoulder to receive the experimental tube and support the mounting assembly. In

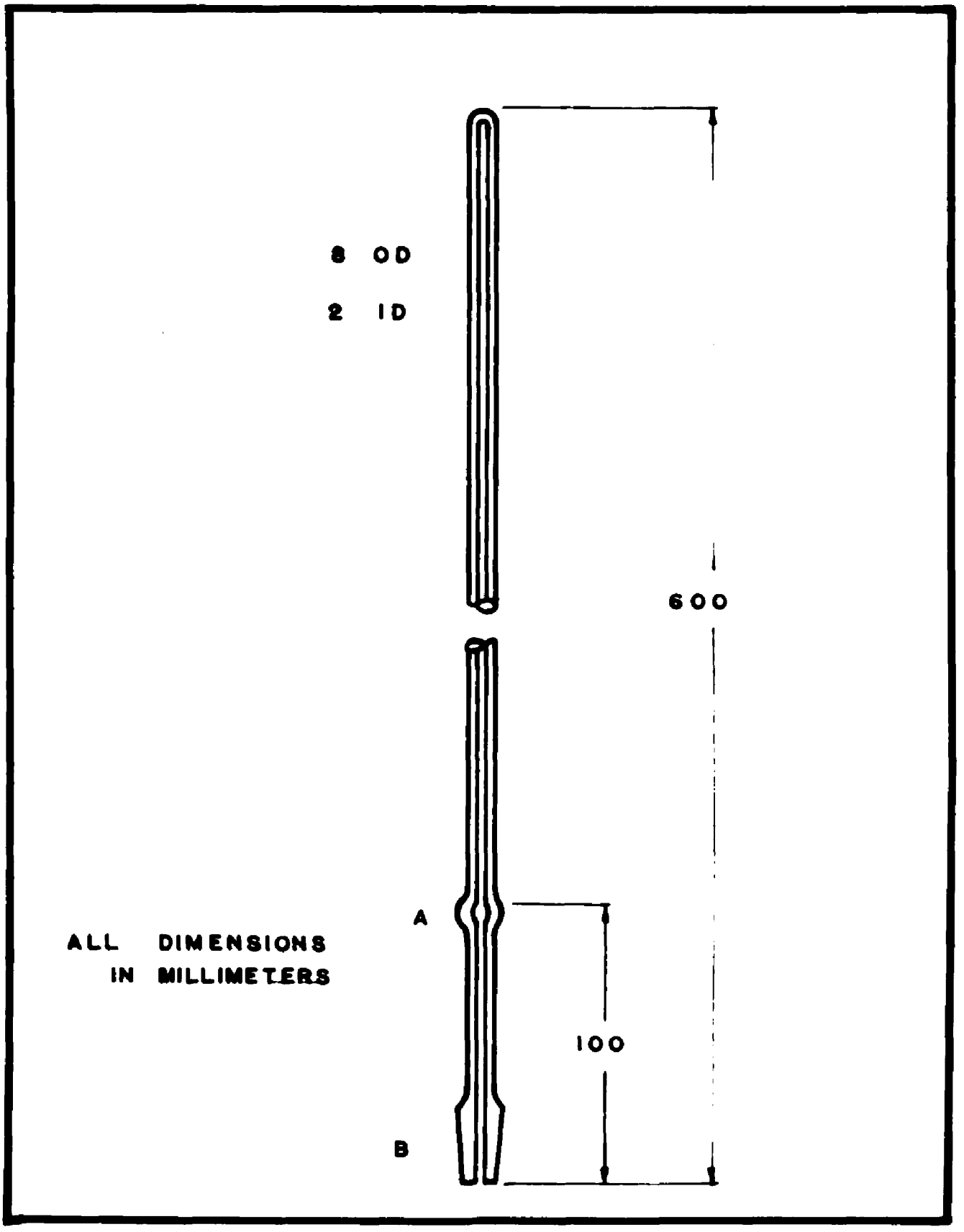

Fig. 4. Experimental Tube

order to maintain an absolutely pressure tight seal between the glass tube and the metal block, a series of rubber and metal gaskets as indicated in Figure 5 were used.

The assembly labeled (A) supplied the main mechanical support for the experimental tube by seating on the shoulder of the compressor block. Shown in partial detail in Figure 5A, this assembly which also served to properly align the tube, consisted of a two-piece sleeve (J) and (K) supporting a ring (H) split in half and a rubber gasket (L). The split ring was made with an inside diameter of approximately 0.020 inches greater than the diameter of the experimental tube.

When pressure was applied, the thickened collar of the tube was restrained from moving upward by means of leather gasket (B), steel ring (C), rubber gasket (D), steel washer (E), steel gland (F), and steel retaining head (G). By turning down the retaining head the gland and washer compressed the rubber gasket forming a mercury tight seal. The washer was machined to an inside diameter similar to that of the split ring while all other steel pieces were machined to a 0.004 inch tolerance with the compressor block wall and merely a very loose fit inside diameter. The rubber gaskets were machined from laboratory rubber stoppers while frozen by liquid nitrogen and to as close a fit as possible. While operating at higher pressures it was found helpful to insert another washer of teflon

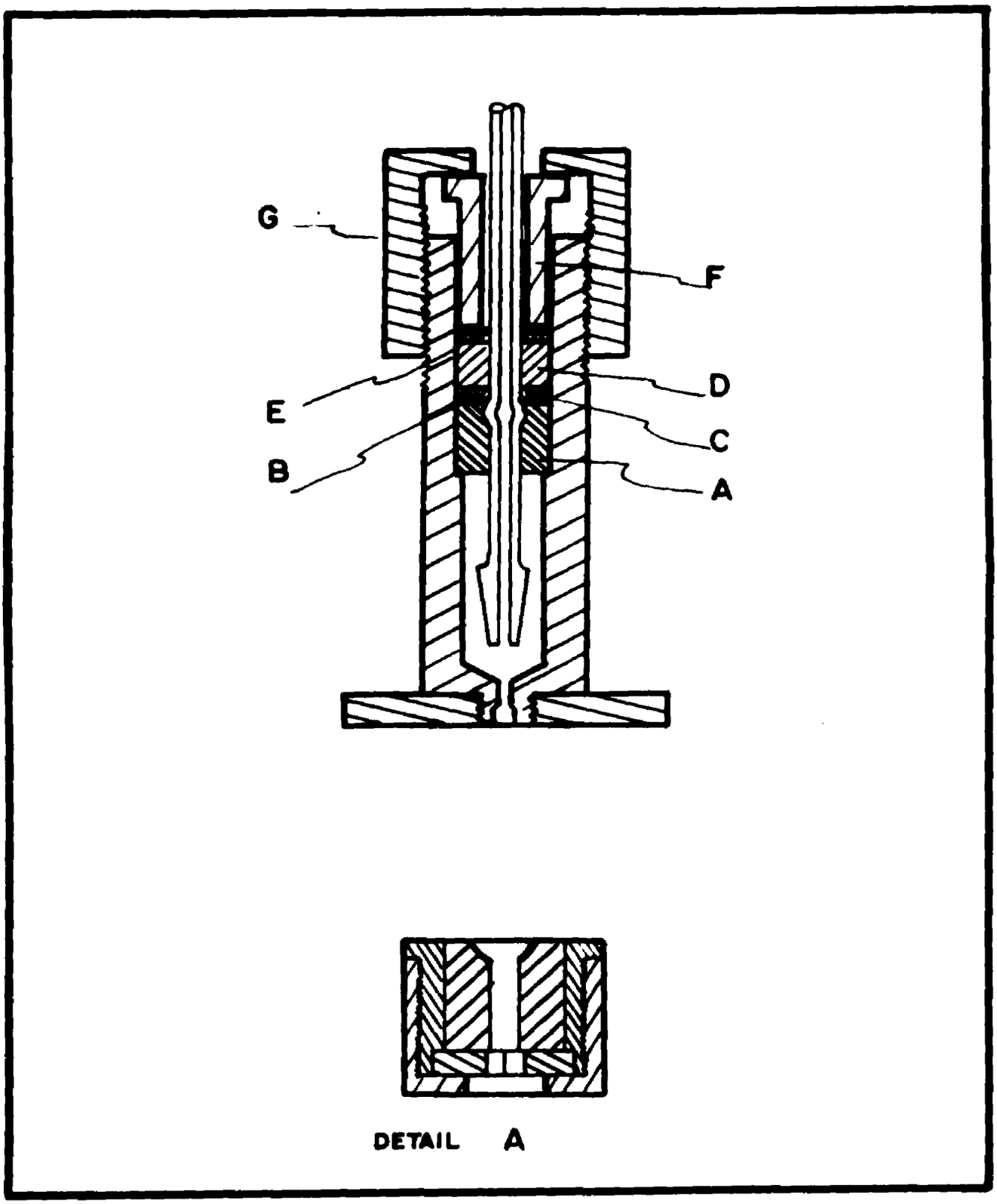

Fig. 5. Compressor Block Assembly

between rubber gasket (D) and washer (E) to minimize the extrusion of rubber around the tube.

Thus the entire assembly simplified proper alignment and eliminated shearing stresses to the experimental tube by having no rigid metal to glass contact.

The Complete Apparatus

Figure 6 is a schematic diagram of the entire apparatus as assembled for use.

Pressure was applied to the sample hydraulically by means of mercury and oil and regulated chiefly by the oil compressor piston. The oil booster pump and the mercury compressor piston were used to regulate the proper quantities of the respective hydraulic fluids. This adjustment was made during the insertion of the experimental tube into the compressor block. The proper amount of mercury or oil to be added or removed was determined by a maximum-minimum mercury level indicator originally constructed by Hoekelman (12). The mercury level indicator consisted of a well made of mild steel into which was inserted two low voltage probes operating from an OA4 vacuum tube to control a relay to two indicating lamps. The level indicator also served as a warning device for leaks in the system which were not observable otherwise.

The pressure in the system was indicated by a bourdon pressure gauge with a range of zero to 5000 psi. The gauge

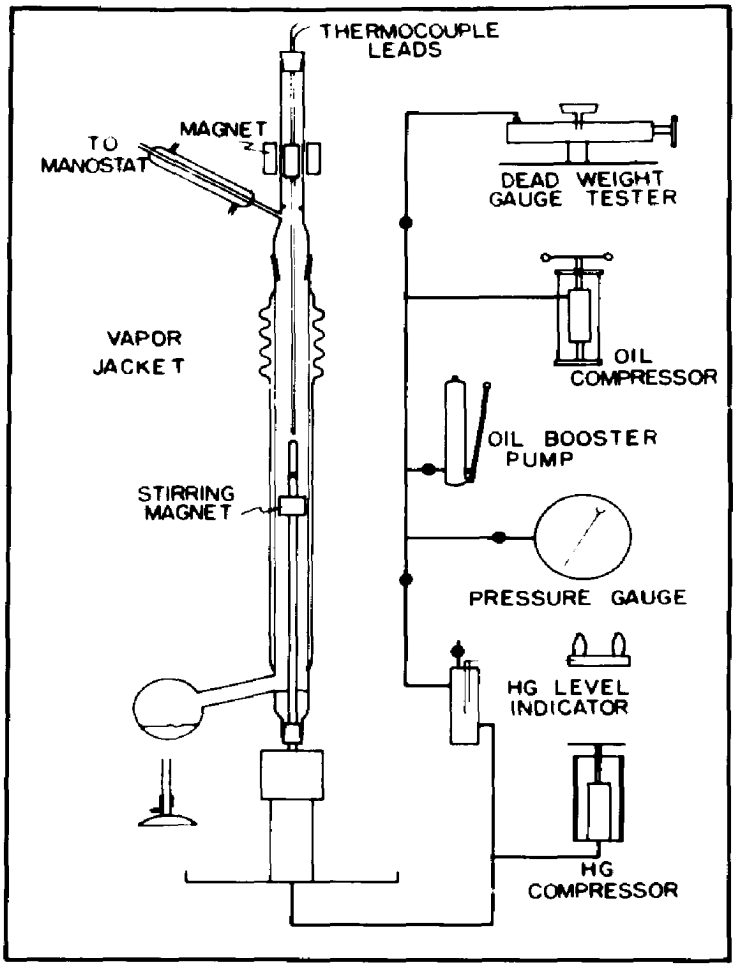

Fig. 6. Schematic Diagram of Assembled Apparatus

was calibrated (Appendix A) periodically and found to be well within its claimed accuracy of ± 0.1 per cent of the full scale reading. Although the smallest scale devision was 5 psi, repeated point calibrations during the entire experimental program showed that an ultimate accuracy of ± 1 psi was readily observable.

The dead weight gauge tester was made a part of the apparatus in order to check not only for permanent set of the bourdon tube but also for hysteresis effects.

In Figure 6 the experimental tube is shown surrounded by a vapor thermostat. The pressure within the jacket and thus the temperature of the condensing vapor, was controlled by means of stopcocks which allowed air to enter into or be evacuated from the vapor thermostat system. During the course of the experiment it was found necessary to use only two different boiling fluids, i.e., diphenyl ether for the temperature range 200°C to 250°C and mercury for the range 250°C to 354°C. Because of the toxicity of mercury vapors the thermostated tube was mounted in a ventilated hood and the mercury heated with a small bunsen burner.

The temperature was measured by means of an iron-constantan thermocouple in conjunction with a potentiometer which could detect readily a temperature change of 0.02°C. The temperature maintained by the thermostat and indicated by the thermocouple was estimated to have the conservative

accuracy of ± 0.05°C. The calibration of the thermocouple system is described in Appendix A.

To hasten the attainment of equilibrium, the sample was stirred by means of a steel ball inside the experimental tube. Stirring was accomplished by moving a large permanent magnet mounted at the top and outside the jacket as shown in Figure 6. The large magnet moved an iron core inside the vapor jacket and from which was suspended a small permanent magnet surrounding the experimental tube. The small magnet moved the steel ball through the sample.

As an aid to the observation of the phase changes a light of variable intensity was mounted behind the vapor jacket and a small telescope was mounted in front.

Details of the construction of the individual components of the apparatus or in the case of commercially available equipment, the names of the manufacturers, can be found in Appendix D.

Purification and Properties of the Components

The water used in the experiments was freshly prepared conductivity water obtained from The Ohio State University reagents laboratory and contained less than 0.1 ppm of solids as sodium chloride.

Although measurements of the vapor pressure of degassed samples of water were made, they were used as a guide toward learning the proper manipulation of the apparatus by comparing the results with the "Steam Tables"

of Keenan and Keyes (19). In other words, the sample purity and the "Steam Tables" were considered a standard for the experiment. A deviation of the measured vapor pressure of water from the standard was indicative of the accuracy and amounted to ± 1 psi.

The benzene used was prepared from one liter of Baker's reagent grade benzene which carried the A.C.S. specification approval. The benzene was twice rectified from phosphorous pentoxide in a six-foot packed column using a 20 to 1 reflux ratio. Approximately the middle half cut was taken each time as product. Several pure degassed samples of benzene were prepared and their vapor pressures to the critical point measured. The values of the critical temperature and critical pressure were 288.7°C and 710 psia, respectively, as compared with 288.7°C and 709.2 psia, respectively, from the work of Nevens (25).

Loading the Experimental Tube

The loading of a sample was basically a high vacuum degassing operation followed by the quantitative transfer of the components, benzene and water, in the vapor phase into the experimental tube. The glass apparatus used was that of Kay (18) and is shown in Figure 7.

With an experimental tube containing a hair capillary probe mounted on the apparatus at (D), the entire system

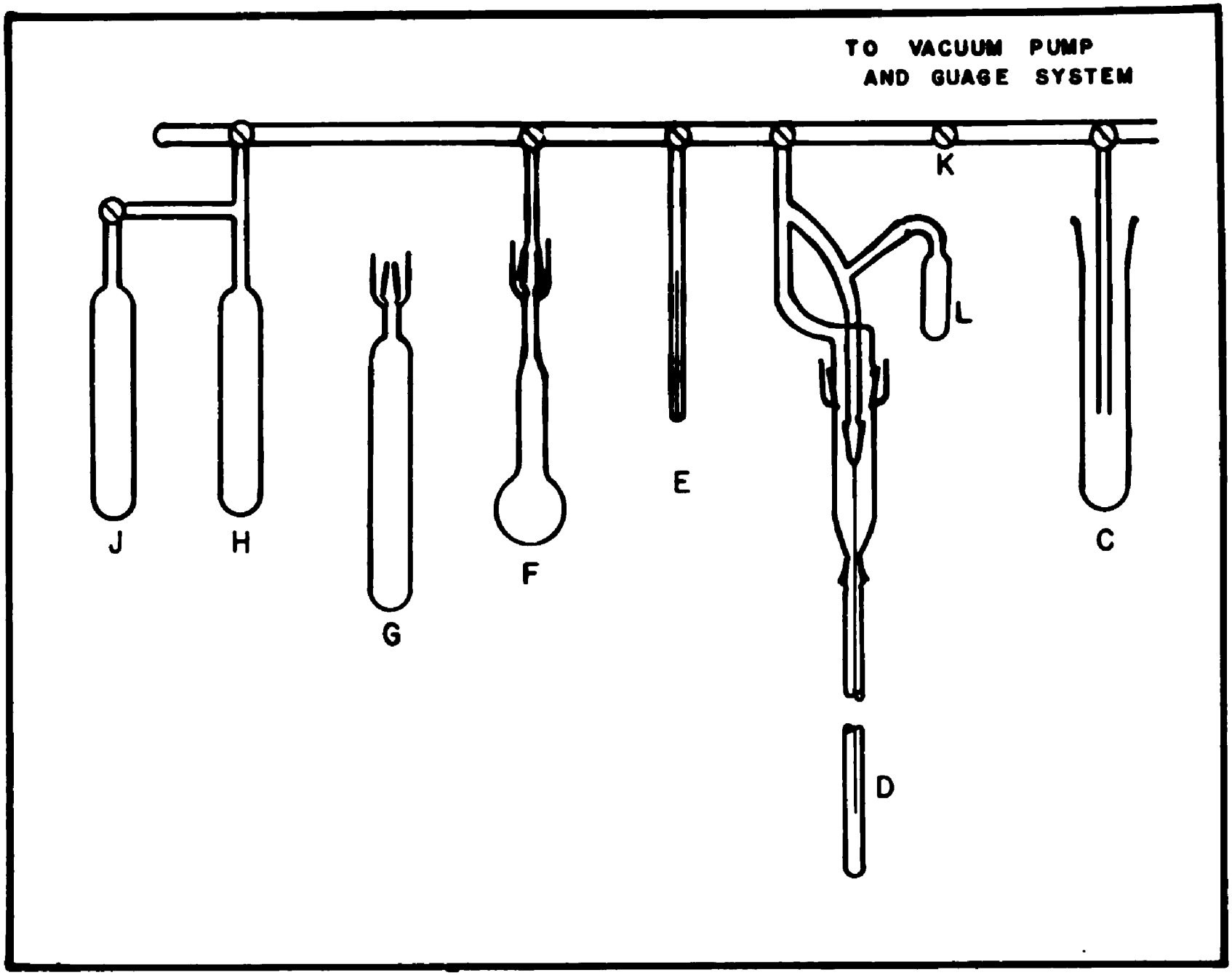

Fig. 7. Loading Apparatus

was evacuated by means of a mechanical vacuum pump in series with a mercury diffusion pump to less than 0.1 micron of mercury pressure. With a vacuum tight system assured, bulb (G) containing about 3 cc of benzene was fixed to the apparatus by means of a mercury sealed tapered glass joint. The benzene was frozen with a cold trap containing dry ice and acetone and the bulb evacuated. After closing valve (K), the cold trap was moved to bulb (J) causing the benzene to transfer by a simple distillation process. Upon completion of the transfer, the system was again pumped free of all liberated gases. Thereafter the benzene was alternately transferred between bulbs (H) and (J) and pumped free of noncondensable gas. This operation was completed six times.

The water was degassed simultaneously with the benzene by a different procedure. Bulb (F) containing about 5 cc of water was mounted on the apparatus in place of bulb (G). During the transfer operation of the benzene between bulbs (H) and (J) the remainder of the system including the bulb containing the water was evacuated. A dry ice-acetone cold trap was used to freeze the water and hold it under high vacuum. Then while the benzene bulbs were being pumped, the cold trap was removed from the water bulb and the ice allowed to melt. When there was no visible boiling of the liquid water upon opening the stopcock (F) to high vacuum, the water was assumed to be completely degassed.

Upon completion of the degassing operation the measuring capillary (E) and the experimental tube were purged and rinsed with liquid benzene. The benzene in bulb (H) was allowed to melt and vapors were condensed in the two capillaries with an ice water trap. With the proper adjustment of stopcocks and the source of benzene refrozen the capillaries were pumped dry. The purge benzene was collected at the liquid nitrogen trap (C). This operation was repeated four times.

The actual preparation of the experimental sample followed. The measuring capillary which had been previously calibrated (Appendix A) was first partially filled with liquid benzene and allowed to come to an arbitrary but constant temperature of a cold water bath. The benzene was then evaporated to a predetermined level. After liquid and vapor equilibrium was established, the length of the liquid filled capillary was measured by means of a cathetometer reading to $\pm$ 0.05 mm. The benzene was then quantitatively transferred to the experimental tube trapped with liquid nitrogen.

By means of a similar procedure an exact quantity of water was measured and transferred to the experimental tube. By rotating bulb (L) mercury was poured through the hair capillary probe displacing upward all the remaining space in the experimental tube. The tube was immediately removed from the loading apparatus and with the

hair capillary removed mounted in the compressor block.

From the measurements of the length and the temperature the volume of liquid of each component was determined. To these volumes were added the equivalent liquid volume of each component contained in the measuring capillary as vapor (Appendix B). In general, the overall size of the sample was 0.036 cc. This size sample was sufficiently large for the observation of dense phase changes and at the same time did not seriously limit the number of observations of phases changes of low density. With the sample size fixed the limit of accuracy of the numerical value of composition was $\pm$ 0.002 weight fraction.

Experimental Procedure

With the experimental tube containing a sample of known composition mounted in the compressor block and with the vapor jacket and stirring rig completely assembled, heat was applied and the thermostatic fluid allowed to boil for a period of about one hour prior to making actual measurements. Having established a constant temperature the sample was compressed until a second or third phase either appeared or disappeared. In most instances it was easier to establish the point of phase change by compression rather than decompression of the sample with one notable exception, namely, observations made in the large retrograde areas.

For each observed point the E M F of the thermocouple, the pressure reading of the gauge, and the level of the mercury column in the experimental tube were recorded. A model data sheet was devised in order to simplify the application of corrections to these basic measurements. Shown in Table II is a sample of this data sheet on which are indicated by asterisks the primary measurements.

The significance of the items in the table are as follows:

*1. The E M F generated by the thermocouple.

2. The deviation of the actual E M F of the thermocouple from the reference chart (Appendix A, Figure 14) as determined by standardization.

3. The value of E M F on the chart from which to read the corresponding temperature.

4. The value of the temperature as indicated by the nearest 0.1 millivolt (Appendix A, Table VI).

5. The interpolated fraction of temperature.

6. The true temperature of the thermostat.

*7. The height of the mercury meniscus in the experimental tube above an arbitrary datum plane near the base of the compressor block.

8. A constant correction for the difference in hydrostatic head between the datum plane near the base of the compressor block and the center of the bourdon tube in the pressure gauge.

9. The contribution to the pressure indicated on the gauge by hydrostatic head. Sum of 7 and 8.

10. The contribution to the pressure indicated on the gauge due to the vapor pressure of mercury in the experimental tube.

11. and 12. The accumulated negative correction to apply to the gauge reading. Sum of 9 and 10.

*13. The actual reading on the gauge.

14. A deviation correction to apply to the gauge determined by calibration. (Appendix A, Figure 13)

15. The true gauge pressure.

*16. The barometric pressure.

17. The absolute pressure at the gauge. Sum of 15 and 16.

18. The absolute pressure exerted by the sample. Sum of 17 and 12.

These data (Appendix C) were plotted on a large graph while they were being taken in order to test immediately their consistency and to establish the direction of the particular phase boundary under observation. The time required to correct and plot a datum point was usually sufficient time to establish a new temperature level in the thermostat. No general rule was followed in determining the size of the increment of the temperature change from point to point.

TABLE II: Sample Data Sheet

Corrected data on Sample Number 9

	Observation No.	438
#1.	Observed EMF (m.v.)	18.228
2.	- correction	-.042
3.	Chart EMF	18.270
4.	Whole degrees	334.06
5.	Fractional degrees	1.26
6.	Temperature ^{o}C	335.3
	Pressure	
#7.	Relative Hg head (mm)	596
8.	- reference correction	97
9.	Hydrostatic head	499
10.	Hg vapor pressure (mm)	509
11.	Total negative correction (mm)	1008
12.	Total negative correction (psi)	19.5
#13.	Gauge reading (psi)	2550
14.	- correction	0
15.	Gauge pressure (psig)	2550
#16.	Barometric pressure (psia)	14.4
17.	Absolute pressure @ gauge (psia)	2564.4
18.	Absolute sample pressure (psia)	2545

EXPERIMENTAL DATA

The pressure at the liquid and vapor phase boundaries of fifteen mixtures of benzene and water were determined within the temperature range from 200°C to 357°C. The smoothed data for increments of 100 psi of pressure for twelve of the mixtures and for the three-phase curve are presented in Table III. The same smoothed data for increments of 5°C of temperature are presented in Table IV.

Also indicated in these tables are the values of the unique states of each mixture noted as follows: the vaporization critical point (VC), the maximum temperature for the coexistence of vapor and liquid ($VL-T_m$), the maximum pressure for the coexistence of vapor and liquid ($VL-P_m$), the maximum three-phase temperature and pressure ($3p_m$), and the maximum temperature for two liquid phases ($2L-T_m$).

All values of the three-phase curve and its extension are common to all mixtures for temperatures and pressures below the values indicated as the maximum three-phase temperature and pressure ($3p_m$) or indicated as the maximum temperature for two liquid phases ($2L-T_m$).

The values in the tables marked with an asterisk are extrapolated values. The raw data for each mixture are given in Appendix C, Table VIII. Included in the Appendix C, Table IX, are a series of observations in temperature and pressure which represent points where the refractive index

for two liquid phases was the same.

Vapor pressures of the pure components were also measured but were used primarily as a check on the experimental procedure as explained in the previous section.

TABLE III: The Pressure-Temperature Relations at the Phase Boundaries of the System Benzene-Water at Equal Intervals of Pressure

Pressure psia	Temp. °C	
All compositions: 3-phase and extensions		
300	180.7	
400	195.6	
500	206.7	
600	216.8	
700	225.7	
800	233.8	
900	241.1	
1000	247.7	
1100	253.8	
1200	259.3	
1300	264.6	
1364	268.3	VC
1400	269.8	
1500	274.8	
1600	279.6	
1700	284.2	
1800	288.8	
1900	293.3	
2000	297.7	
2100	301.0	
2200	303.9	
2300	306.2	$2L-T_m$

Pressure psia	Temp. °C	
Composition: 5.3 wt% water		
300*	201.2	
400*	217.7	
500*	230.8	
600*	241.7	
700*	251.2	
800*	259.3	
900	266.5	
1000	271.6	
1025	272.3	
1050	272.9	
1085	273.2	$VL-T_m$
1100	273.0	
1115	272.7	
1127	272.2	VC
1140	271.5	
1150	270.3	$VL-P_m$
1125	266.0	
1100	263.6	
1000	254.7	
900	245.1	
800	235.2	
720	227.5	3 p_m
Composition: 9.4 wt% water		
300*	192.6	
400*	209.0	
500*	222.3	
600*	233.4	
700*	243.1	
800	250.9	
900	258.7	
1000	265.2	
1100	269.6	
1150	270.8	
1170	271.0	$VL-T_m$
1185	270.7	
1207	269.7	VC
1215	269.3	
1220	268.5	$VL-P_m$
1215	267.5	
1200	265.6	
1100	256.9	
1000	249.1	
924	242.5	3 p_m

TABLE III (continued)

Pressure psia	Temp. °C	
Composition: 19.4 wt% water		
300*	181.8	
400*	196.9	
500*	209.4	
600*	220.1	
700*	229.3	
800*	237.5	
900	244.8	
1000	251.1	
1100	257.1	
1200	262.5	
1300	266.9	
1322	267.5	
1334	267.8	$VC-T_m$
1340	267.6	$VL-P_m$
1330	267.0	
1320	266.2	
1300	265.0	
1278	263.5	3 p_m
Composition: 25.7 wt% water		
400*	197.7	
500*	209.0	
600*	218.6	
700*	227.4	
800*	235.3	
900*	242.0	
1000	248.0	
1100	253.8	
1200	259.3	
1212	260.0	Azeo.
1300	264.9	
1350	267.2	
1361	267.6	VC
1355	267.5	3 p_m
Composition: 29.9 wt% water		
300*	186.8	
400*	200.5	
500*	211.8	
600*	221.6	

Pressure psia	Temp. °C	
Composition: 29.9 wt% water (continued)		
700*	230.3	
800	237.4	
900	244.8	
1000	250.8	
1100	256.7	
1200	262.3	
1300	267.6	
1400	272.6	
1500	277.1	
1600	281.1	
1650	282.7	
1665	283.1	$VL-T_m-P_m$
1670	282.8	$2L-T_m$
1675	282.4	
1700	282.1	
1800	281.3	
1900	280.3	
2000	279.4	
2100	278.5	
2200	277.7	
2300	276.8	
Composition: 36.1 wt% water		
300*	192.6	
400*	207.1	
500*	218.4	
600*	228.6	
700*	237.3	
800*	244.9	
900*	252.3	
1000	258.7	
1100	264.8	
1200	270.3	
1300	275.4	
1400	280.3	
1500	284.8	
1600	288.8	
1700	292.5	
1800	295.6	
1900	298.2	
2000	299.6	$VL-T_m$
2015	299.5	

TABLE III (continued)

Pressure psia	Temp. °C	
Composition: 36.1 wt% water (continued)		
2025	299.1	$VL-P_m$
2015	298.4	
1998	298.0	
1992	297.5	$2L-T_m$
2000	296.8	
2050	295.3	
2100	294.3	
2200	293.2	
2300	292.5	
2400	292.0	
2500	291.7	
2600	291.3	
2700	291.2	
Composition: 50.9 wt% water		
300*	204.8	
400*	218.9	
500*	230.3	
600*	240.1	
700*	248.7	
800*	256.8	
900*	263.0	
1000*	269.4	
1100*	275.3	
1200*	280.5	
1300	286.1	
1400	290.8	
1500	295.2	
1600	299.3	
1700	303.2	
1800	306.9	
1900	310.4	
2000	313.7	
2100	316.7	
2200	319.4	
2300	320.8	
2390	321.6	$VL-T_m$
2425	321.4	
2443	320.4	$VL-P_m$
2425	318.0	

Pressure psia	Temp. °C	
Composition: 50.9 wt% water (continued)		
2400	316.1	
2350	312.2	
2325	310.2	
2305	307.5	
2302	306.0	$2L-T_m$
2325	303.2	
2400	300.7	
2500	299.1	
2600	298.5	
2700	298.0	
2800	297.7	
2900	297.6	
Composition: 64.9 wt% water		
300*	210.6	
400*	224.8	
500*	236.2	
600*	246.3	
700*	255.8	
800*	262.4	
900*	269.4	
1000*	275.9	
1100*	281.7	
1200*	287.3	
1300*	292.4	
1400*	297.6	
1500	302.0	
1600	306.2	
1700	310.1	
1800	313.9	
1900	317.6	
2000	320.8	
2100	324.2	
2200	327.2	
2300	330.0	
2400	332.5	
2500	334.5	
2600	335.9	
2650	336.2	$VL-T_m$

TABLE III (continued)

Pressure psia	Temp. °C	
Composition: 64.9 wt% water (continued)		
2675	336.1	
2686	335.2	$VL-P_m$
2675	333.7	
2600	328.8	
2500	322.1	
2400	315.2	
2325	309.7	
2301	306.4	$2L-T_m$
2325	303.5	
2400	301.0	
2500	299.2	
2600	298.3	
2700	297.5	
2800	297.0	
2900	296.7	
Composition: 69.9 wt% water		
2711	336.1	VC
Composition: 78.0 wt% water		
300*	214.0	
400*	228.1	
500*	240.1	
600*	250.1	
700*	259.3	
800*	267.0	
900*	274.4	
1000*	281.1	
1100*	287.0	
1200*	293.1	
1300*	298.2	
1400*	301.5	
1500*	307.8	
1600*	312.6	
1700	317.2	
1800	320.9	
1900	324.6	
2000	328.0	

Pressure psia	Temp. °C	
Composition: 78.0 wt% water (continued)		
2100	331.4	
2200	334.7	
2300	337.7	
2400	340.6	
2500	343.3	
2600	346.0	
2700	348.3	
2800	350.1	
2890	351.0	$VL-T_m$
2920	350.4	$VL-P_m$
2918	350.0	VC
2900	348.6	
2800	342.3	
2700	337.2	
2600	332.3	
2500	327.3	
2400	322.2	
2300	316.7	
2200	310.3	
2125	303.4	
2118	301.7	$2L-T_m$
2125	300.1	
2200	297.5	
2300	295.4	
2400	294.4	
2500	293.6	
Composition: 88.3 wt% water		
2500	335.2	
2400	330.6	
2300	325.8	
2200	320.8	
2100	315.4	
2000	309.3	
1900	302.3	
1800	293.4	
1763	287.5	$2L-T_m$
1775	285.7	
1800	284.9	
1900	283.6	
2000	282.8	
(3110)	(365)	(VC est.)

TABLE III (continued)

Pressure psia	Temp. °C
Composition: 94.0 wt% water	
2875	357.4
2800	354.7
2700	351.2
2600	347.6
2500	344.0
2400	340.2
2300	337.7
2200	332.2
2100	327.8
2000	323.3
1900	318.4
1800	312.9
1700	306.5
1600	299.3
1500	291.8
1400	283.8
1300	273.4
1215	260.2 3 p_m

TABLE IV: The Pressure-Temperature Relations at the Phase Boundaries of the System Benzene-Water at Equal Intervals of Temperature

Temp. °C	Pressure psia	
All compositions: 3-phase and extension		
180	295	
185	326	
190	360	
195	395	
200	438	
205	484	
210	531	
215	580	
220	633	
225	691	
230	752	
235	816	
240	885	
245	958	
250	1038	
255	1123	
260	1212	
265	1307	
268.3	1364	VC
270	1404	
275	1504	
280	1610	
285	1716	
290	1825	
295	1934	
300	2070	
305	2240	
306.4	2302	$2L-T_m$
Composition: 5.3 wt% water		
200*	287	
205*	320	
210*	351	
215*	383	
220*	418	
225*	452	
230*	495	
235*	536	
240*	582	
245*	630	
250*	682	
255	742	
260	807	
265	875	
270	963	
272	1014	
273	1055	
273.2	1085	$VL-T_m$
273	1100	
272.2	1127	VC
271	1147	
270.3	1150	$VL-P_m$
268	1140	
265	1115	
260	1060	
255	1003	
250	951	
245	900	
240	848	
235	797	
230	745	
227.5	720	$3\ p_m$
Composition: 9.4 wt% water		
195*	315	
200*	343	
205*	375	
210*	409	
215*	443	
220*	482	
225*	522	
230*	568	
235*	619	
240	673	
245	730	
250	788	
255	850	
260	919	

TABLE IV (continued)

Temp. °C	Pressure psia	
Composition: 9.4 wt% water (continued)		
265	996	
270	1116	
271.0	1170	VL-T_m
270.5	1190	
269.7	1207	VC
269.5	1211	
269	1217	
268.5	1220	VL-P_m
268	1219	
265	1193	
260	1136	
255	1075	
250	1011	
245	952	
242.5	924	3 p_m
Composition: 19.4 wt% water		
180*	290	
185*	320	
190*	353	
195*	388	
200*	419	
205*	463	
210*	505	
215*	551	
220*	598	
225*	652	
230*	708	
235*	769	
240	835	
245	903	
250	981	
255	1063	
260	1150	
265	1255	
267	1305	
267.5	1322	
267.8	1334	VC-T_m
267	1330	
266	1316	

Temp. °C	Pressure psia	
Composition: 19.4 wt% water (continued)		
265	1300	
263.5	1278	3 p_m
Composition: 25.7 wt% water		
200*	417	
205*	462	
210*	510	
215*	561	
220*	615	
225*	671	
230*	732	
235*	797	
240*	869	
245	947	
250	1031	
255	1120	
260	1212	Azeo
265	1303	
266	1320	
267	1338	
268	1356	
268.3	1361	VC
Composition: 29.9 wt% water		
190*	320	
195*	360	
200*	395	
205*	438	
210*	483	
215*	531	
220*	583	
225*	640	
230*	698	
235	762	
240	828	
245	906	
250	985	
255	1070	

TABLE IV (continued)

Temp. °C	Pressure psia	
Composition: 29.9 wt% water (continued)		
260	1158	
265	1250	
270	1346	
275	1452	
280	1572	
283.1	1665	$VL-T_m-P_m$
282.8	1670	$2L-T_m$
282.5	1674	
282	1710	
281	1830	
280	1938	
277	2275	
Composition: 36.1 wt% water		
195*	315	
200*	348	
205*	385	
210*	426	
215*	470	
220*	515	
225*	565	
230*	618	
235*	676	
240*	737	
245*	802	
250*	871	
255	943	
260	1020	
265	1103	
270	1193	
275	1290	
280	1391	
285	1504	
290	1632	
295	1778	
299	1944	
299.6	2000	$VL-T_m$
299.5	2015	
299.4	2019	
299.3	2022	
299.2	2024	

Temp. °C	Pressure psia	
Composition: 36.1 wt% water (continued)		
299.1	2025	$VL-P_m$
298.8	2022	
298.6	2018	
298.4	2015	
298.2	2006	
298.0	1998	
297.5	1992	$2L-T_m$
297	1997	
296	2025	
294	2133	
292	2405	
Composition: 50.9 wt% water		
205*	297	
210*	331	
215*	369	
220*	410	
225*	452	
230*	498	
235*	548	
240*	601	
245*	656	
250*	717	
255*	783	
260*	855	
265*	930	
270*	1012	
275*	1096	
280*	1183	
285	1278	
290	1382	
295	1494	
300	1616	
305	1747	
310	1888	
315	2040	
320	2240	
321.6	2390	$VL-T_m$
321	2439	
320.4	2443	$VL-P_m$
320	2441	

TABLE IV (continued)

Temp. °C	Pressure psia	
Composition: 50.9 wt% water (continued)		
315	2583	
310	2327	
306	2302	2L-T_m
304	2310	
303	2327	
300	2429	
Composition: 64.9 wt% water		
215*	327	
220*	363	
225*	402	
230*	442	
235*	487	
240*	535	
245*	585	
250*	642	
255*	703	
260*	766	
265*	835	
270*	911	
275*	990	
280	1073	
285*	1158	
290*	1249	
295*	1348	
300	1455	
305	1570	
310	1697	
315	1830	
320	1972	
325	2125	
330	2300	
335	2527	
336.2	2650	VL-T_m
336.1	2675	
335	2685	
330	2618	
325	2542	
320	2467	
315	2395	

Temp. °C	Pressure psia	
Composition: 64.9 wt% water (continued)		
310	2327	
308	2307	
306.4	2301	2L-T_m
305	2306	
303	2335	
300	2460	
Composition: 69.9 wt% water		
336.1	2711	VC
Composition: 78.0 wt% water		
225*	378	
230*	417	
235*	456	
240*	500	
245*	546	
250*	597	
255*	652	
260*	711	
265*	773	
270*	840	
275*	912	
280*	985	
285*	1066	
290*	1151	
295*	1238	
300*	1331	
305*	1428	
310*	1531	
315	1645	
320	1773	
325	1912	
330	2057	
335	2210	
340	2376	
345	2560	
350	2795	
351.0	2890	VL-T_m
350.4	2920	VL-P_m

TABLE IV (continued)

Temp. °C	Pressure psia	
Composition: 78.0 wt% water (continued)		
350.0	2918	VC
345	2845	
340	2757	
335	2654	
330	2552	
325	2452	
320	2357	
315	2272	
310	2195	
305	2136	
301.7	2118	2L-T_m
300	2125	
298	2182	
295	2334	
293.7	2513	
Composition: 88.3 wt% water		
365	3110	VC (est)
335	2497	
330	2386	
325	2282	
320	2183	
315	2138	
310	2011	
305	1935	
300	1870	
295	1815	
290	1772	
287.5	1763	2L-T_m
287	1764	
286	1770	
285	1795	
284	1865	
282.8	2000	

Temp. °C	Pressure psia	
Composition: 94.0 wt% water		
357	2863	
355	2807	
350	2667	
345	2526	
340	2376	
335	2268	
330	2149	
325	2037	
320	1932	
315	1835	
310	1752	
305	1679	
300	1608	
295	1542	
290	1475	
285	1412	
280	1360	
275	1313	
270	1273	
265	1240	
260.2	1215	3 p_m

RESULTS

Presentation

From the graphically smoothed data presented in Tables III and IV a series of crossplots were prepared in order to interpret more fully the nature of the phase behavior. Figure 8 is the pressure-temperature plot of the basic data on which the individual continuous curves represent the phase boundaries of a mixture of fixed overall composition. From this plot were obtained the smoothed data of the above mentioned tables. A curve for the mixture containing 25.7 weight per cent water is not shown because it lies so close to the three-phase curve. Also not shown are the curves for three other mixtures which were investigated only in the region of their criticals. The vapor pressure curves of the pure components are taken from the literature.

Figure 10 depicts the temperature-composition phase boundaries at progressively increasing constant pressure levels. Similarly, Figure 9 shows the pressure-composition phase boundaries at progressively increasing constant temperature levels.

The temperature-composition projection of the three-phase curve and the critical temperatures are shown in Figure 11. Other unique states of the system as a function of composition are noted in the tables of the experimental

data. These values as a function of composition are shown in Figure 12.

Figures 8 through 12 are direct reproductions of the carefully plotted data. However, all values of temperature, pressure, and composition on the coordinates of these reproductions are only approximate where they are written as whole numbers and are intended only as an aid to the coordination of the various figures.

Discussion of errors

A general idea of the precision of all the measurements is given in the description of the apparatus. The experimental accuracy obtained for the measurement of temperature and pressure as proved by the graphical smoothing of the raw data was within the limit of precision for the greater number of data points, namely, ± 1 psi and ± 0.05°C. The scattering of the remainder of the data points was attributed chiefly to the inability of the observer to recognize the exact characteristic of the phase behavior at a given point. The mixture containing 29.9 weight per cent water in the range of 295°C and 2000 psia was an example of this situation. Under these conditions because of the minute quantity of liquid phase present, it was difficult to differentiate a dew point from either a bubble point or a point of complete miscibility.

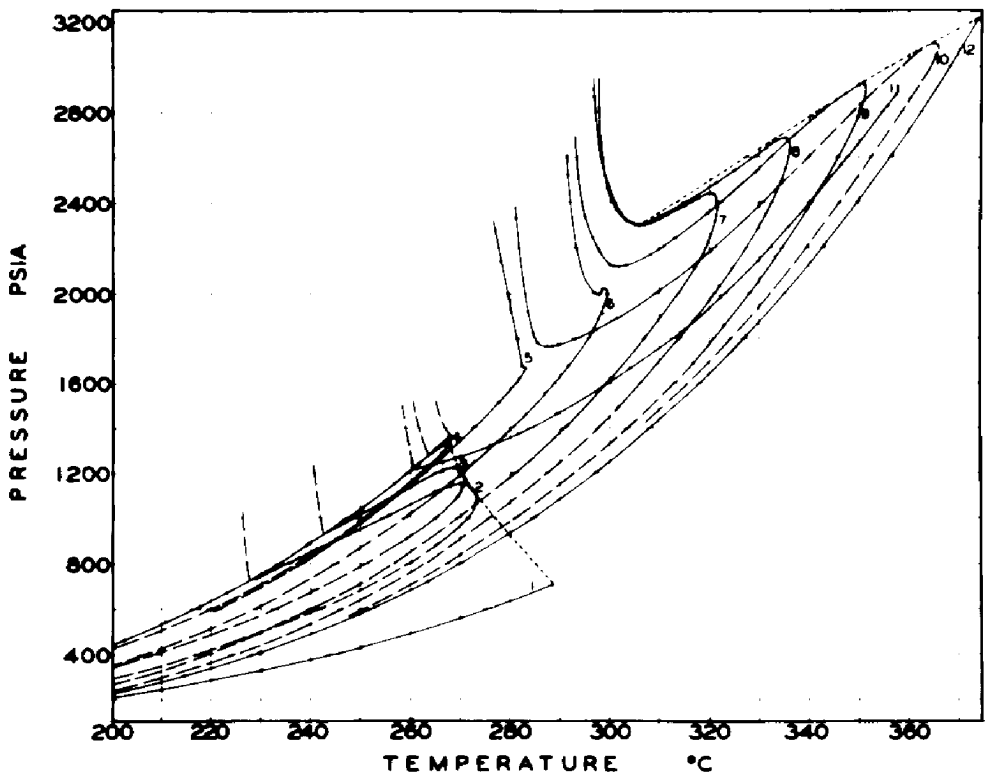

Fig. 8. The Pressure-Temperature Phase Boundaries

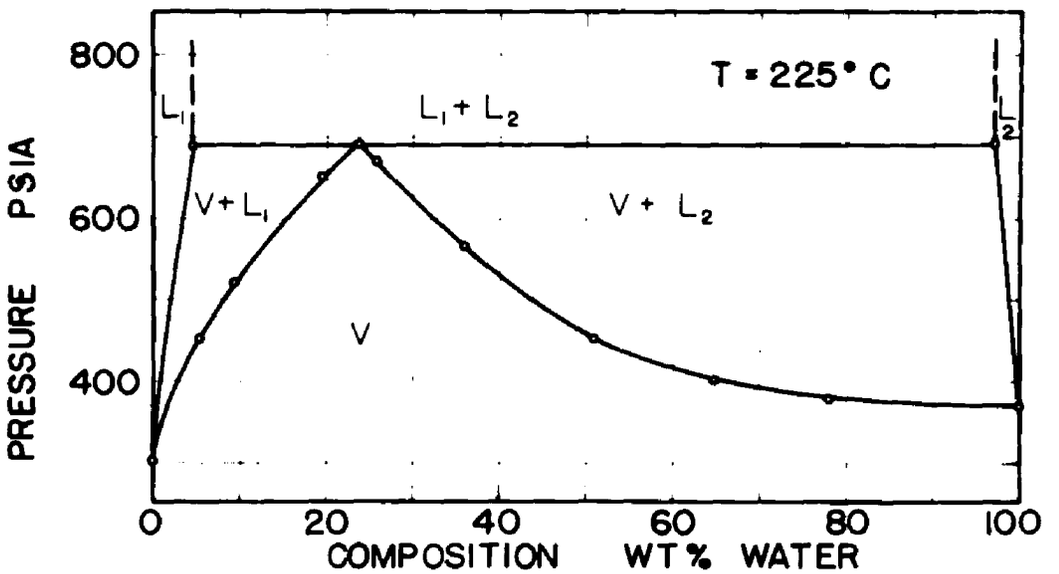

9A

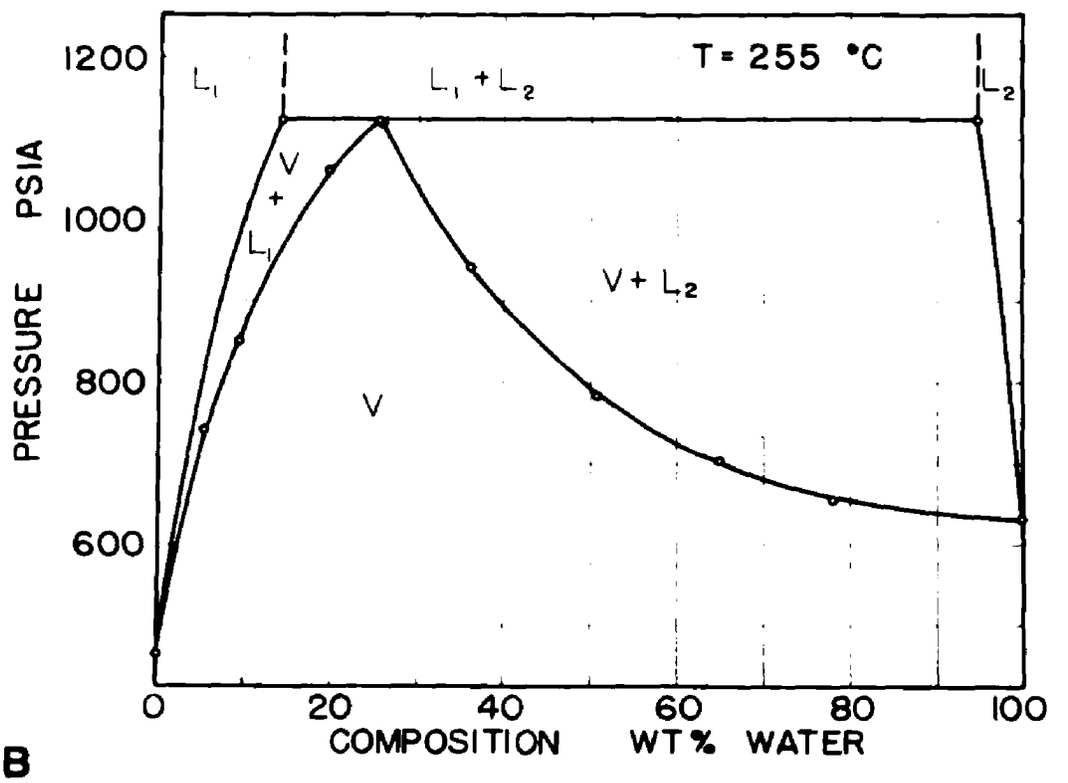

9B

Fig. 9. Isotherms of the System

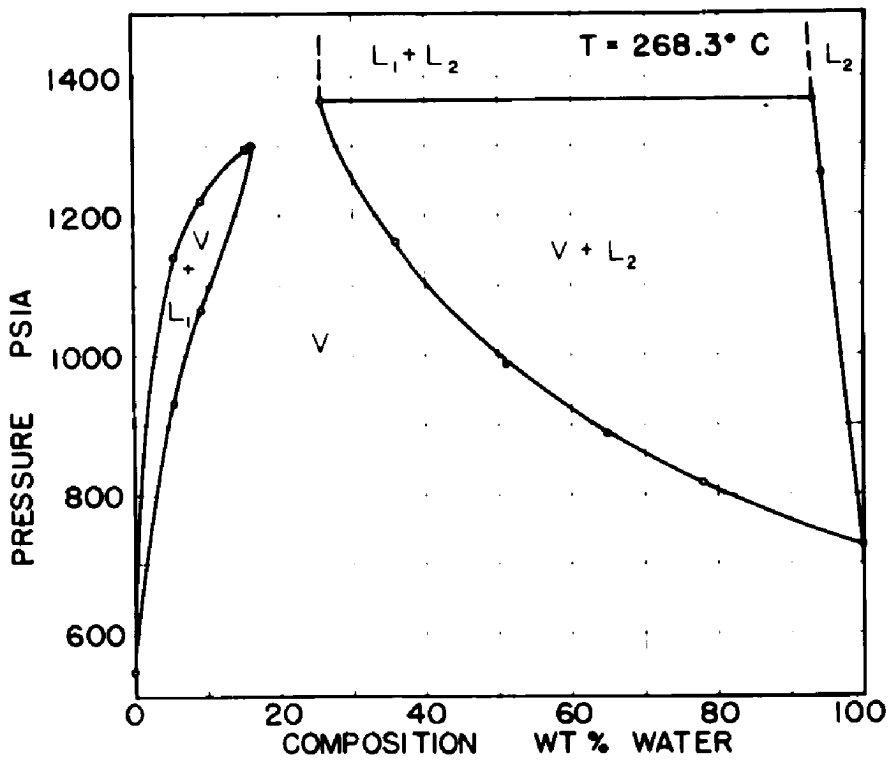

9C

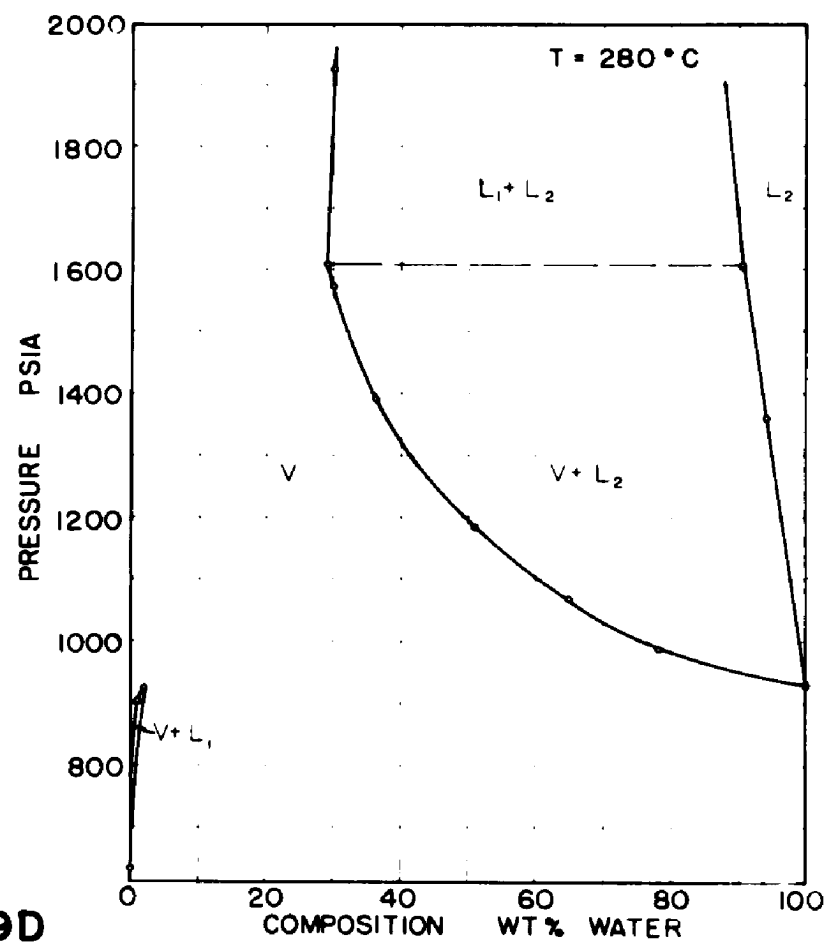

9D

Fig. 9.
(continued)

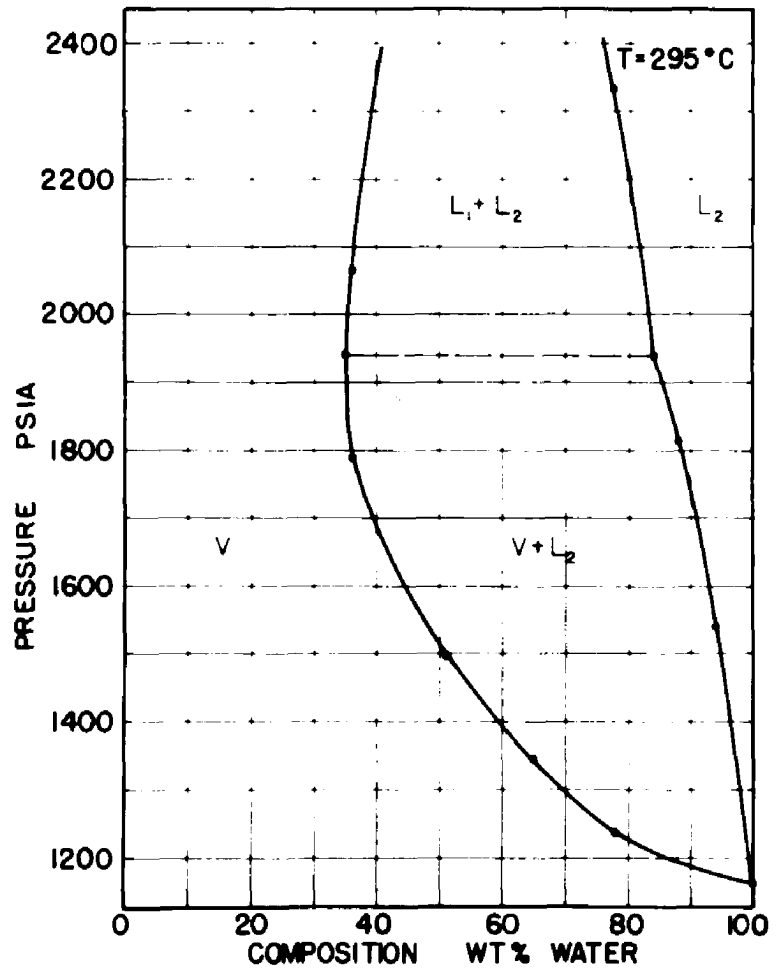

9E

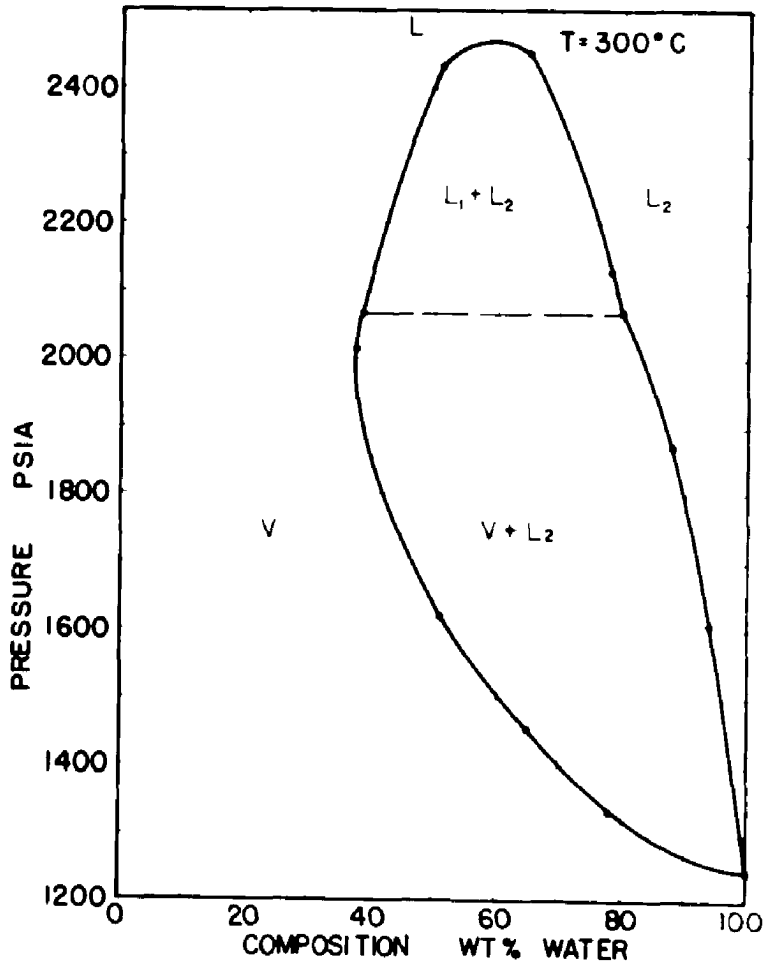

9F

Fig. 9 (continued)

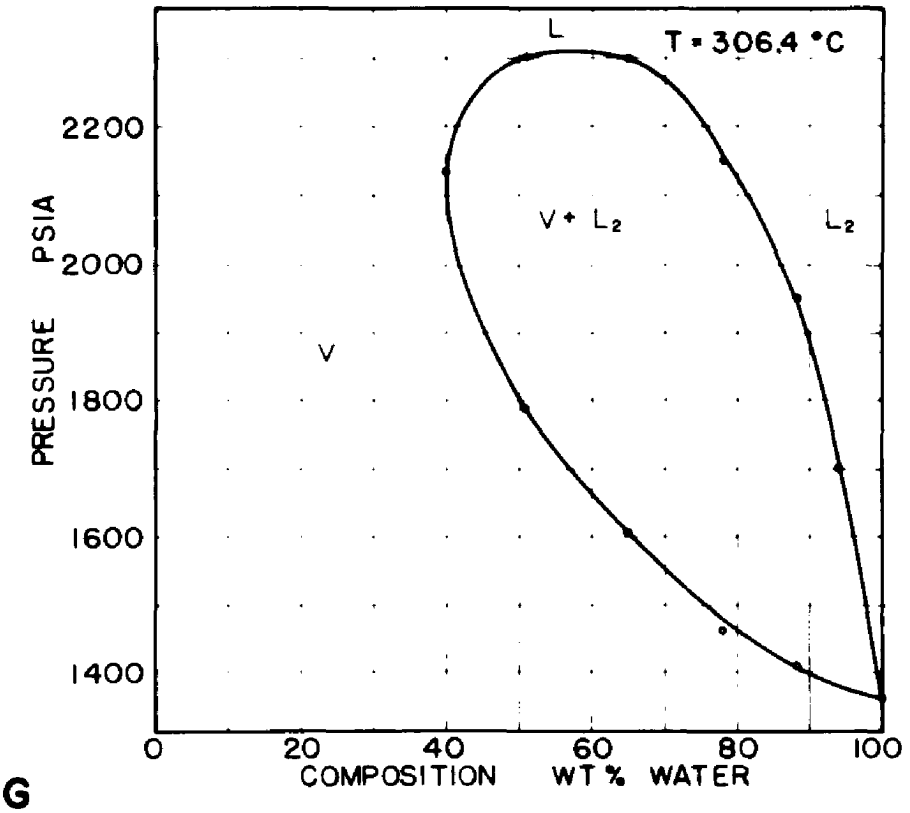

9 G

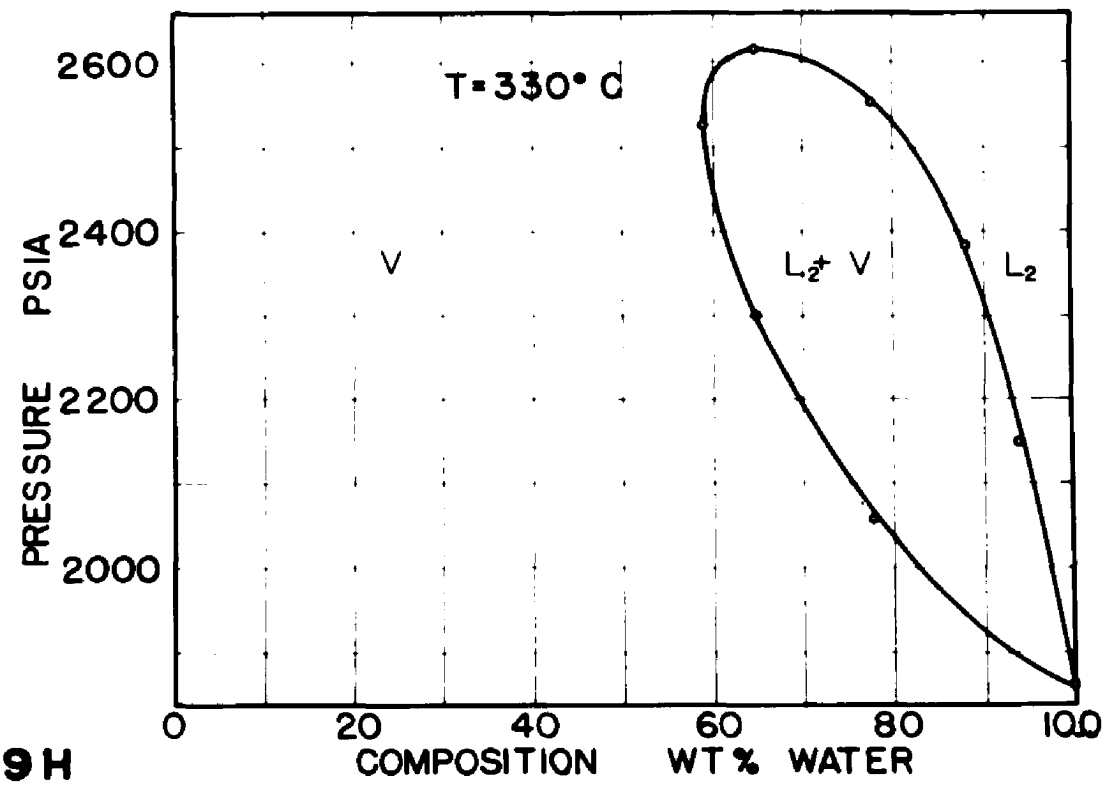

9 H

Fig. 9. (continued)

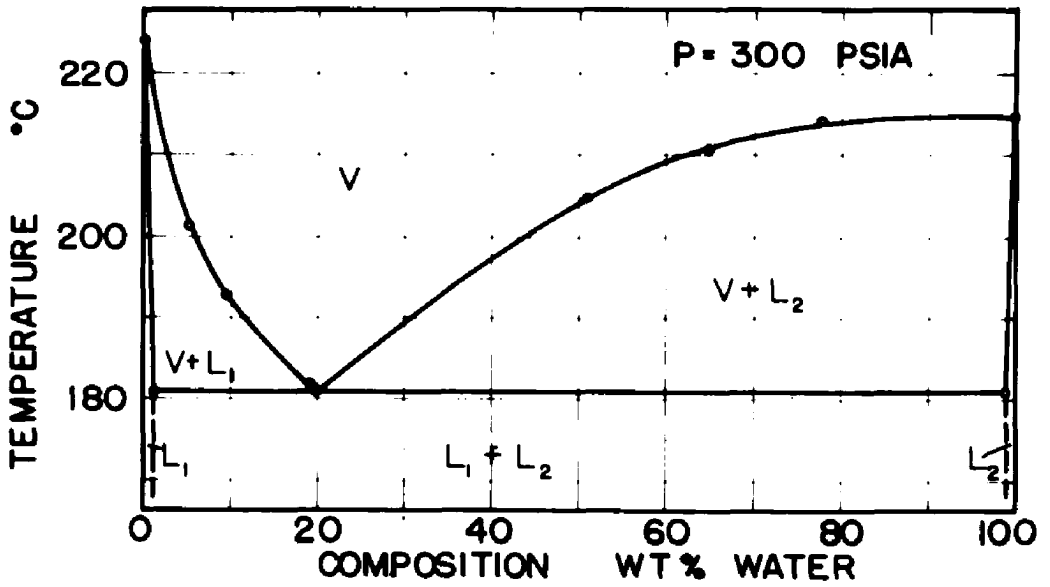

10 A

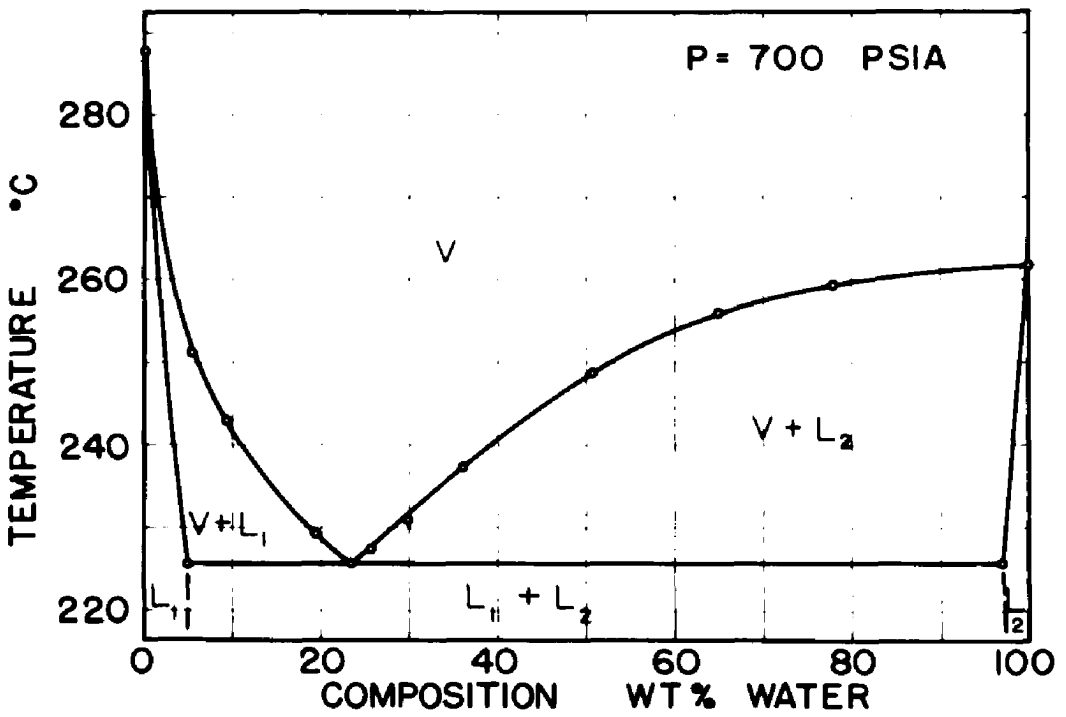

10 B

Fig. 10. Isobars of the System

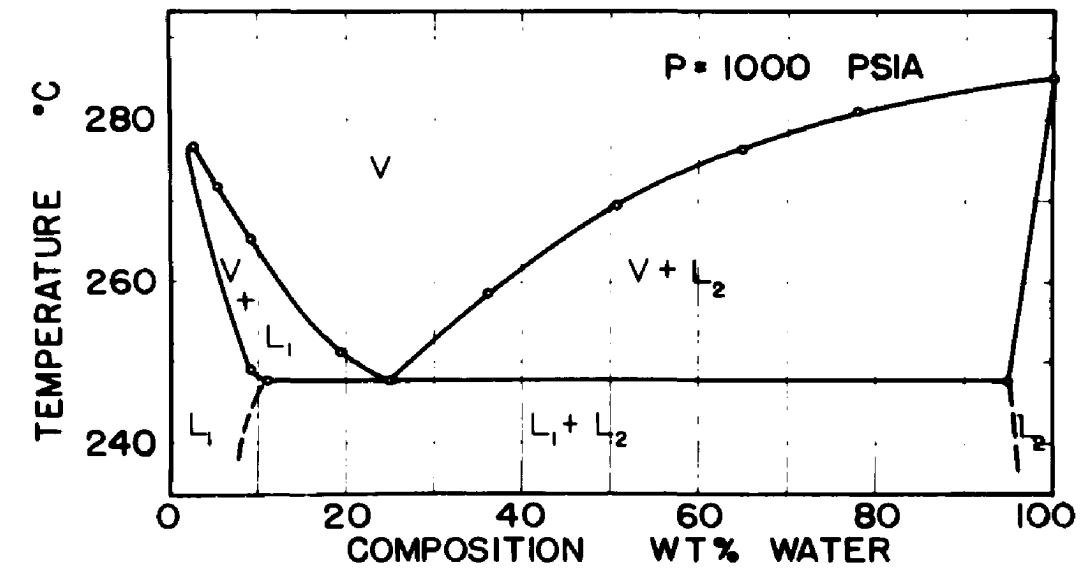

10 C

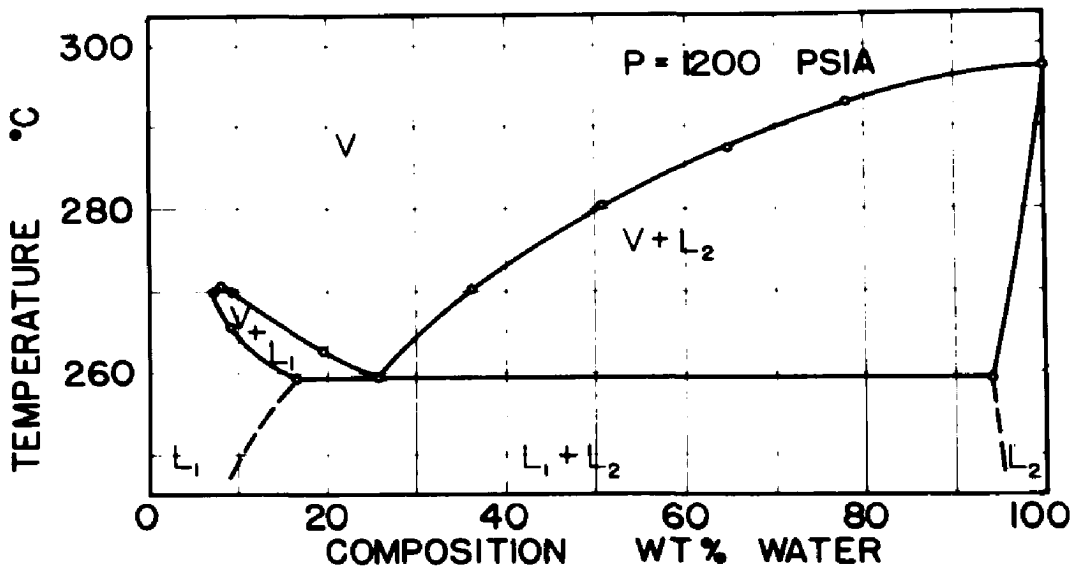

10 D

Fig. 10. (continued)

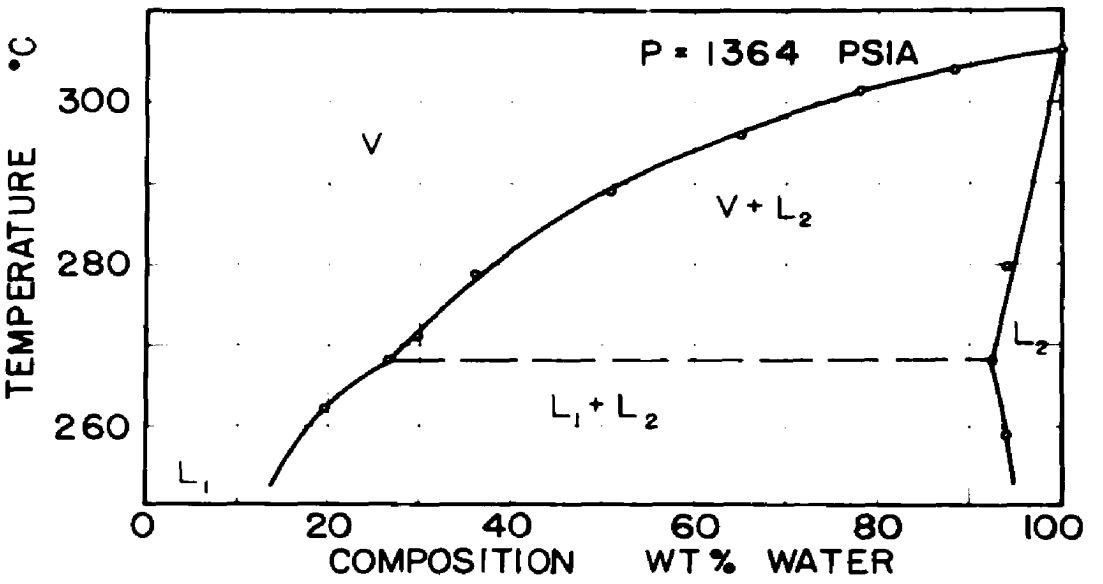

10 E

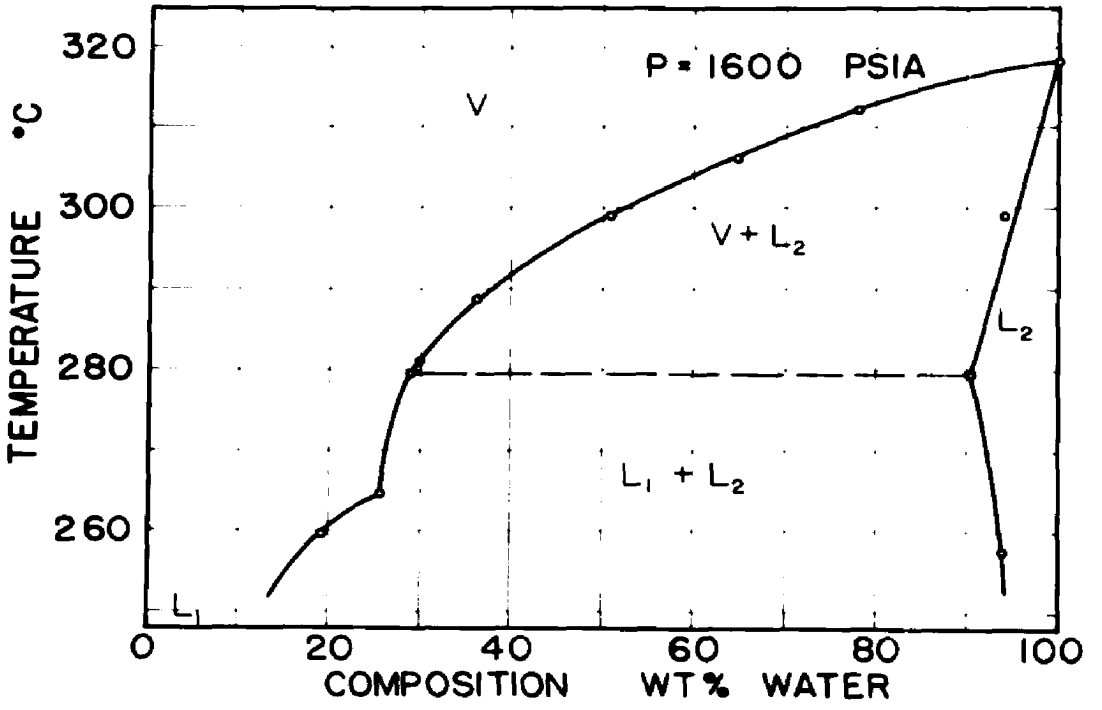

10 F

Fig. 10. (continued)

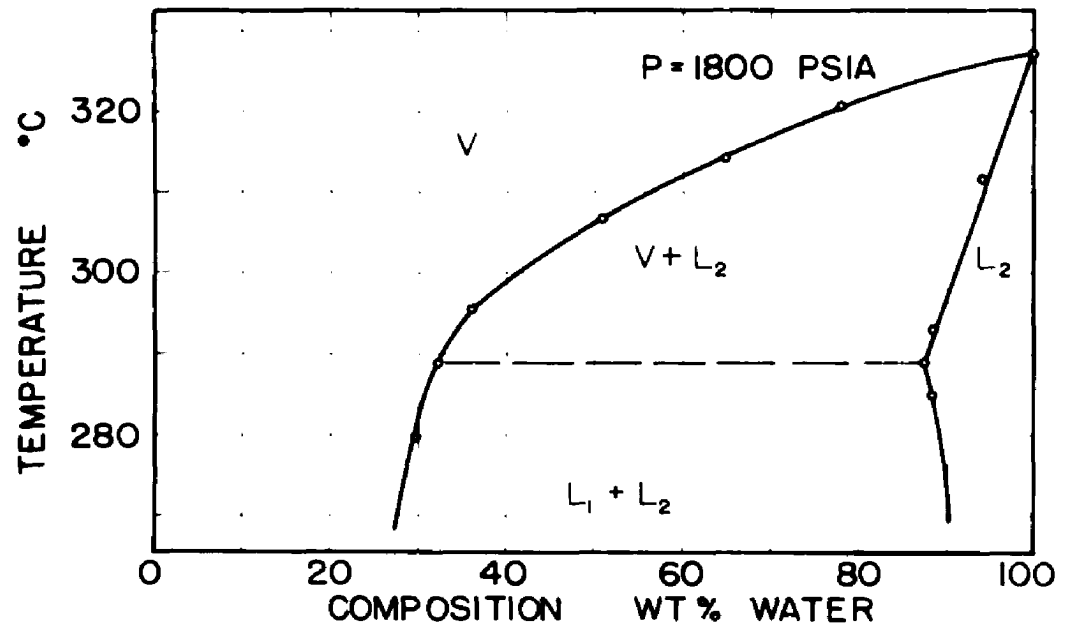

10 G

Fig. 10. (continued)

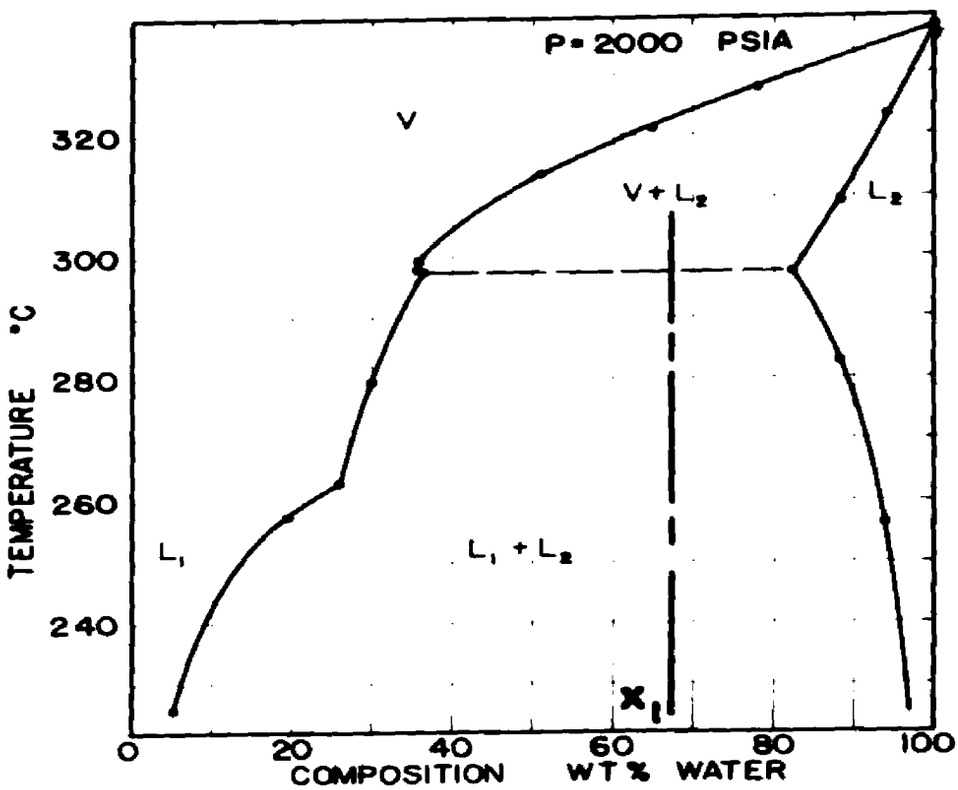

10 H

Fig. 10. (continued)

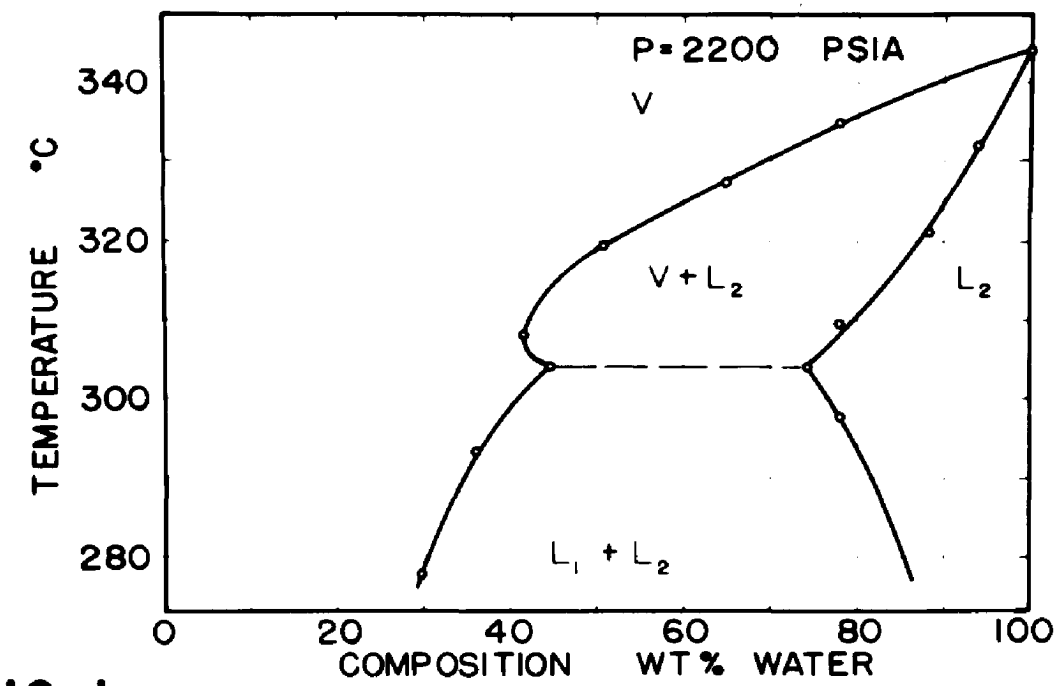

10 J

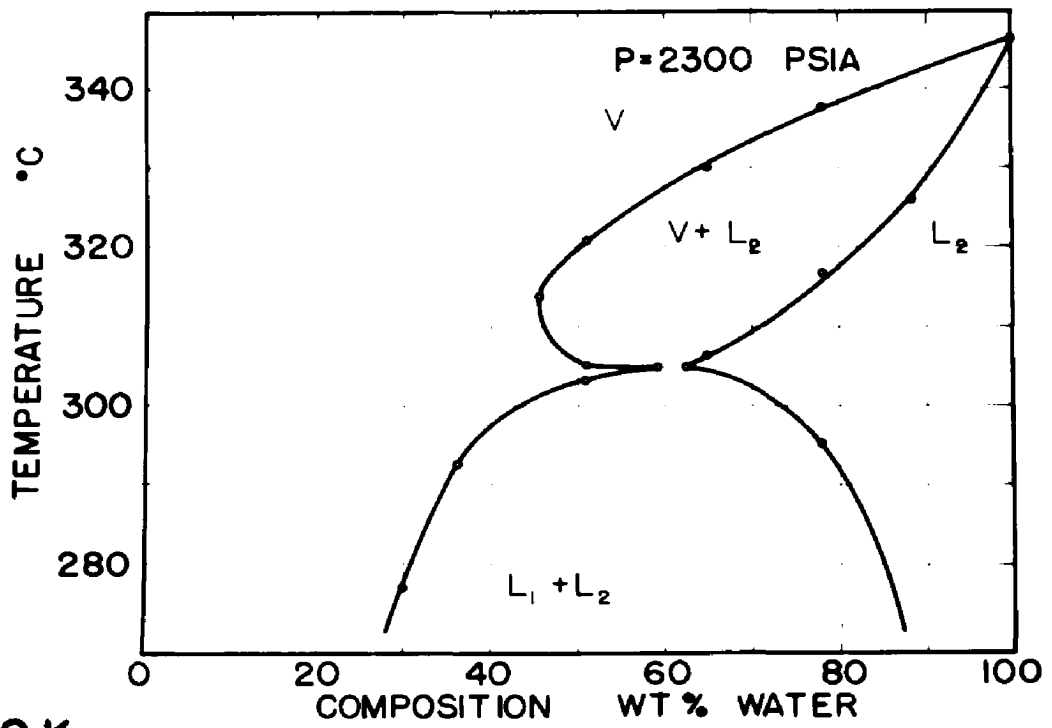

10 K

Fig. 10. (continued)

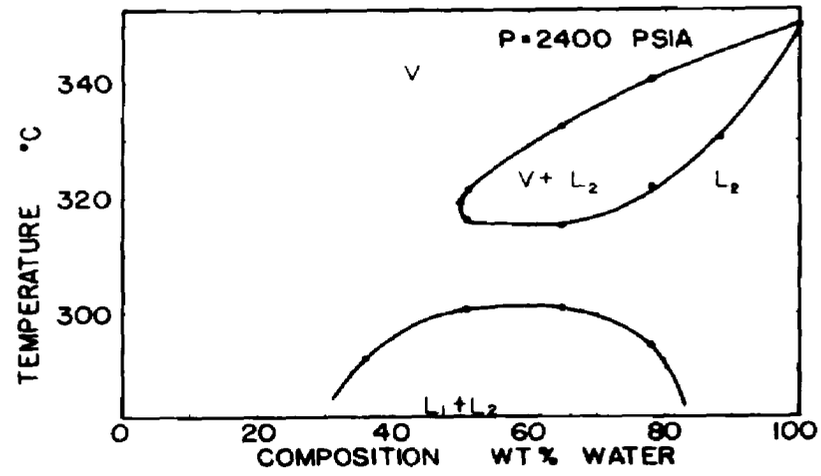

10 L

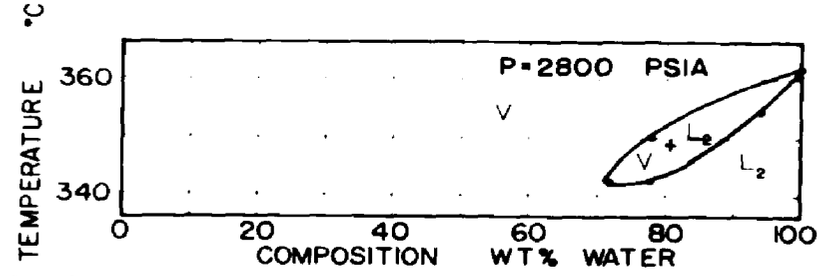

10 M

Fig. 10. (continued)

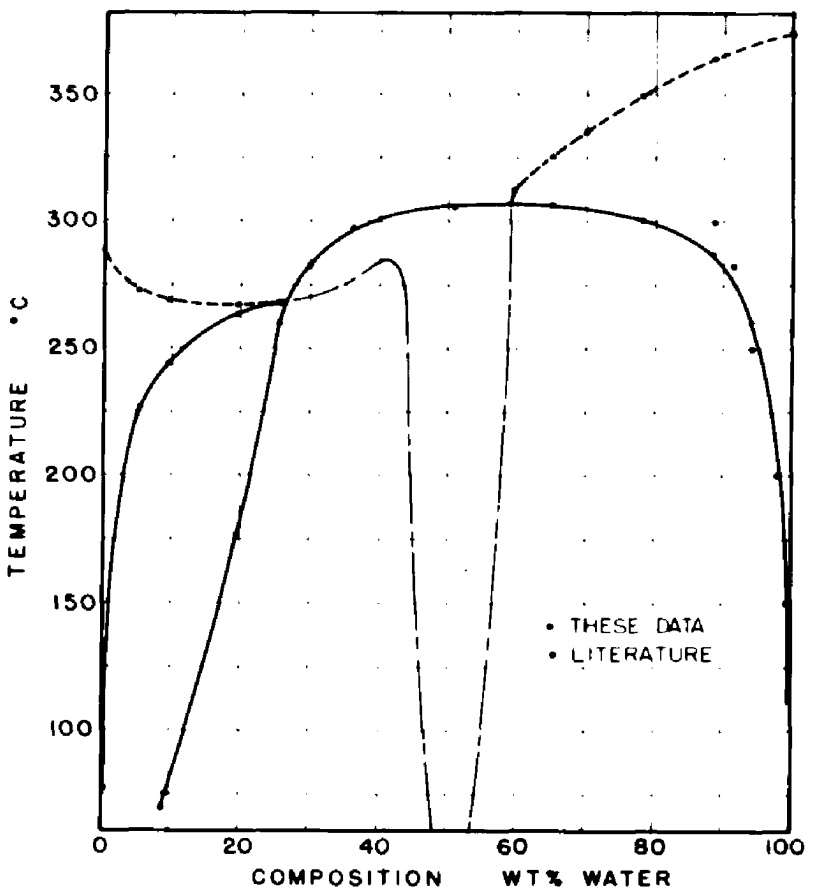

Fig. 11. The Temperature-Composition Projection

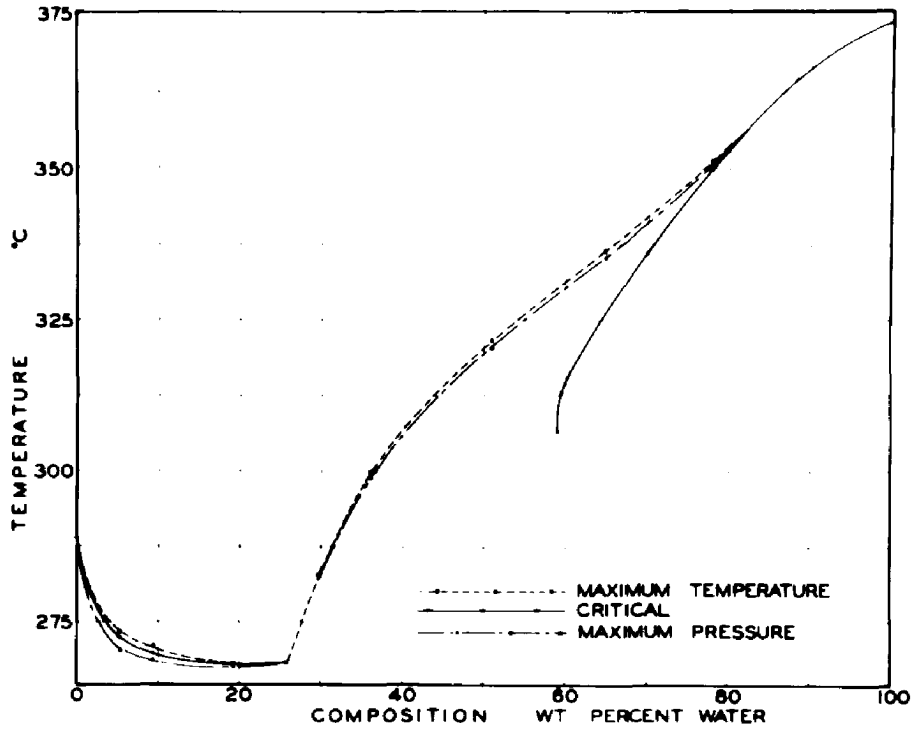

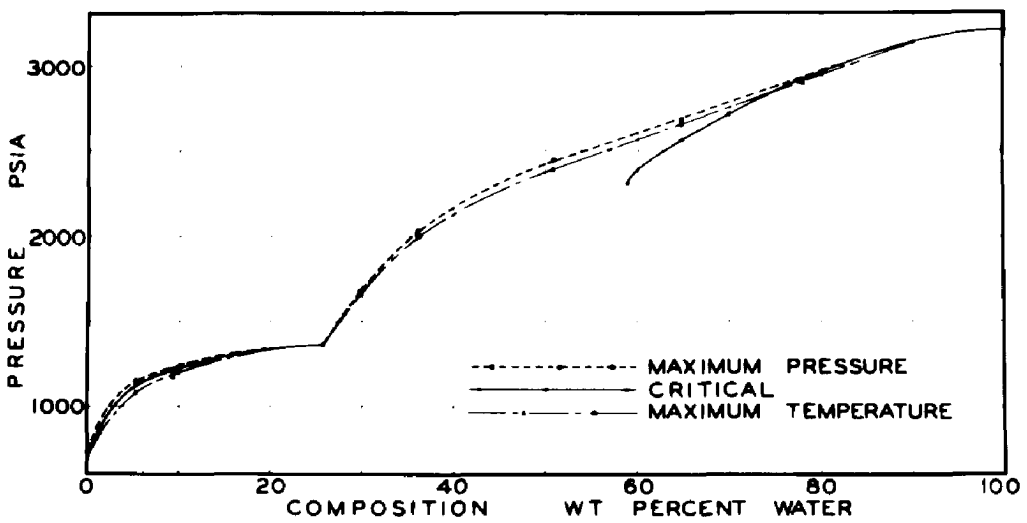

Fig. 12. Unique States of the System

The accuracy of the measurement of the composition was most apparent in the construction of the crossplot sections. Thus sample numbered 3 has been eliminated from consideration because of its lack of consistency with the bulk of the data. For the fourteen other mixtures the compositions were easily within the range of $\pm$ 0.002 weight fraction.

All other deviations of the data points from graphically smooth representation were ascribed to the possible existence of contaminants originating in the course of degassing and sampling. The procedure and manipulation for the elimination of dissolved gases was perfected and proved by the preparation and testing of five samples of pure benzene and two samples of pure water. However, the elimination of possible contamination by dissolved stopcock grease was resolved by compromise. By testing four readily available stopcock greases, a heavy lanolin-based grease was found to be the most effective in resisting the vapor phases of both benzene and water. Although the area of contact between the greased surfaces and the vapors was very small, other factors such as the ambient temperature of the loading apparatus and the duration of the time of contact could very well have been the cause of greater or lesser stopcock grease contamination.

The graphing of the phase boundaries of the benzene-water system was done on rectangular coordinates on which the scales were chosen commensurate with the accuracy of the original data. On all master graphs pressure was represented by a scale of 1 mm to 5 psi, temperature by a scale of 1 mm to 0.25°C, and composition by a scale of 1 mm to 0.5 weight per cent.

Extension of the data

In order to develop more fully the surface of the P-T-x solid, the data have been extended in some cases by a qualified extrapolation. Only into those regions where the nature of the phase behavior had been previously comprehended was extrapolation attempted.

Because of the limited and fixed working volume of the experimental tube there existed a minimum temperature and pressure for each mixture at which the entire sample could be completely vaporized. As a result the measurement of dew points was terminated in the case of all mixtures at a value of temperature and pressure far above the desired lower limit of values. The measured portion of the curves were extrapolated by plotting the logarithm of the absolute pressure versus the reciprocal of the absolute temperature and extending the resulting straight line.

Although this procedure has been found satisfactory in representing the vapor pressure of a pure compound with the same accuracy as this work, it had a serious limitation when applied to benzene-water mixtures, since this system formed an azeotrope. Consequently, on the extrapolation plot the straight line representing the temperature-pressure relation of a fixed vapor composition had to become tangent at a single point with the straight line representing the three-phase curve, if the simple rule used were to apply over the entire length of the dew point curve.

Since only two values of the azeotropic composition of the three-phase vapor composition were actually measured, these values were extended by a more lengthy procedure. First, from the original data a series of T-x plots at constant pressure were prepared. From these plots several more points of the desired vapor composition were determined. These values along with a single value from the literature measured at atmospheric pressure were plotted as the logarithm of the mol composition of the azeotrope versus the absolute temperature and a smooth, slightly convexd curve drawn. Finally, from the results of this plot the vapor branch up to the three-phase critical was constructed on the T-x projection (Figure 11). Although it is reasonably representative of its true path,

the curve as it was originally drawn had to pass through two points 160°C apart on a temperature scale which ranged approximately 200°C.

The same question of error arises with respect to the benzene-rich liquid solubility curve. Since the highest value in temperature for the solubility of water in benzene which was available from the literature was approximately 70°C and the lowest value of solubility temperature measured was 227°C, the intermediate range of that solubility surve was simply drawn on the T-x projection.

A much sought after value was the composition, temperature, and pressure of the critical solution endpoint. To that end after a preliminary perusal of the data on twelve mixtures, two more mixtures in the neighborhood of 60 weight per cent water were prepared. No convincing critical phenomena other than the three-phase critical was observed for these two mixtures. A very thin, flat meniscus separating the two phases indicating the incidence of a single phase was seen, but there was no opalescence.

Since no critical phenomena had been observed for mixtures of high water concentrations, a final attempt was made with a sample containing 70 weight per cent water. A point in temperature and pressure exhibiting marked critical characteristics was found, but opalescence was very weak.

Interpretation

The phase boundaries for the benzene-water system develop in a manner prescribed by its identification with the classic Case IV up to the temperature (268.3°C) of the benzene-rich liquid critical vaporization point. These typical phase boundaries are seen in Figures 9A, 9B, 9C, 10A, 10B, 10C, and 10D. The existence of the island in the P-x section (Figures 9C and 9D) is the result of the negative slope of the critical locus curve. Referring to Figure 8 it can be seen that any P-x section taken in the range of temperatures from the three-phase critical to the critical point of pure benzene will have an island.

In the region of the three-phase critical temperature and pressure there can be detected the subtleties of the evolution of the surface to realign itself so as to continue on in another direction. Significantly, Figure 11 shows the benzene-rich liquid solubility branch going to the vapor branch abruptly at the three-phase critical. There is no smooth, rounded compromise meeting of the two curves. The vapor branch continues directly on above the three-phase critical, having taken on itself the meaning of both branches from which it evolved. Similarly, the critical locus curves (Figures 8 and 11) go through a minimum before reaching the three-phase critical in order to attain a positive slope and be directed toward its ultimate terminal, the critical point of water.

The three-phase curve extended (Figure 8) beyond its critical temperature (268.3°C) to its final endpoint the critical solution temperature (306.4°C) does in effect continue to represent "three-phase" equilibrium. However, the transition of one of the liquid phases to the vapor phase is continuous and is accompanied by no volume change at constant temperature and pressure.

Both the three-phase curve and its extension have the same interpretation. Both parts of the curve represent the limit of miscibility of two phases at the onset of another phase. Thus, the three-phase curve is a series of points which are the limit of solubility of two liquid phases at a temperature and pressure where a vapor phase is just appearing. On the extension of the three-phase curve are points which represent the limit of the solubility of a benzene-rich dense gas or fluid phase and a water-rich liquid phase at a temperature and pressure where the liquid is just beginning to vaporize. However, the dense fluid and the vapor form a homogeneous mixture which is identified as a single phase.

Tracing the phase changes of a mixture of composition x_1 in Figure 10H illustrates the above interpretation. At some low temperature and a pressure of 2000 psia the mixture will exist as two liquid phases. These two liquid phases increase mutually in solubility as the temperature is raised up to approximately 264°C. With further increase

in temperature the benzene-rich phase is no longer identified as a liquid but rather as a dense fluid and the effect of increased temperature is continued increase in solubility of the two phases.

Upon reaching a temperature of 297°C these two phases have reached their maximum solubility which may, in a broad sense, be called the limit of solubility of the gas and liquid. At this temperature the water-rich phase begins to vaporize and the vapor which is formed is completely dissolved in the benzene-rich fluid. By increasing the temperature above 297°C a normal pattern of behavior takes place. In terms of solubility the liquid becomes more soluble in the vapor while the vapor becomes less soluble in the liquid.

Figure 11 outlines completely the solubility relations of the saturated liquids for the system. All mixtures become completely miscible at a temperature of 306.4°C which corresponds to a pressure of 2303 psia. A mixture containing about 59 weight per cent water is deduced as being the composition which will be critical at this point.

Mixtures which still retain two phases at temperatures and pressures above the critical solution point have phase boundaries like normal binary mixtures as shown in Figures 9H, 10L, and 10M.

Discussion of critical phenomena

The locus of critical vaporization points above the critical solution point is shown with qualification. It is believed that mixtures with compositions approaching pure water will display the critical phenomena more convincingly, since such mixtures will be further removed from the existence of a phase already critical. From the appearance of the various diagrams a critical solution point could exist as deduced. This point should lie on a smooth curve representing the locus of all critical points whether they are critical solution points or critical vaporization points. Such a curve could be drawn on Figure 8 and made to resemble the curve of Figure 3. The projection of such a curve into the T-x plane is shown by the long dashed curve in Figure 8 and it may be that the entire long dashed curve represents unstable or unattainable states. It is possible for a portion of this curve to exist, but the case of the miscibility of benzene-water mixtures above the vapor saturation pressure has yet to be proved.

Furthermore, the whole range of critical temperatures from the three-phase vaporization critical up to pure water may represent unstable critical states. There is some evidence in this direction as indicated in "The International Critical Tables" for the system ethyl ether-water for which

it is reported that the upper critical endpoint is essentially that of pure water.

Of greater importance, however, is the fact that the boundary where critical points could exist is established from the point of pure water down to a point represented by 2303 psia, 306.4°C, and 59 weight per cent water. The connection of this latter point with the three-phase critical via unstable or real critical points has yet to be established.

BIBLIOGRAPHY

1. ATACK, D., and SCHNEIDER, W. C. J. Phys. and Coll. Chem., 54, 1323 (1950).

2. BOHON, R. L., and CLAUSSEN, W. F. JACS, 73, 1571 (1951).

3. BRADBURY, E. J., McNULTY, D., SAVAGE, R. L., and McSWEENEY, E. E., IEC, 44, 211 (1952).

4. BUCHNER, E. H. Z. Physik Chem., 56, 257 (1906).

5. CORRUCCINI, A. J., and SHENKER, H. U. S. Bureau of Standards J. of Research, 50, 229 (1953).

6. DODGE, B. F. and LINDROOS, A. E. AIChE Sympos. Ser. No. 3, 48, 10 (1952).

7. DONHAM, W. Ph.D. Dissertation, The Ohio State Univ. (1954).

8. FRANCIS, A. W. IEC, 36, 1096 (1944).

9. GROSSCHUFF, E. Z. Electrochem, 17, 348 (1911).

10. HERINGTON, E. F. J. App. Chem. (Brit.), 2, 19 (1952).

11. HILDEBRAND, J. H. J. Phys. Chem., 17, 1346 (1949).

12. HOEKELMAN, R. MS Dissertation, The Ohio State Univ., (1953).

13. IPATIEFF, G. S., and MONROE, G. S. IEC Anal. Ed., 14, 171 (1942).

14. JAEGER, A. Brennstoff-Chem., 4, 259 (1923).

15. JORIS, G. G. and TAYLOR, H. S. J. Chem. Phys., 16, 45 (1948).

16. KATZ, D. L. and KOBAYASHI, R. IEC, 45, 440 (1953).

17. KAY, W. B. IEC, 30, 459 (1938).

18. KAY, W. B. and DONHAM, W. Chem. Engr. Sci., 1, 1, (1955).

19. KEENAN, J. H. and KEYES, F. G. Thermodynamic Properties of Steam, John Wiley and Sons, Inc., New York (1936).

20. KEEVIL, N. B. JACS, 64, 841 (1942).

21. KUENEN, J. P. Theorie der Verdampfung und Verflussingung von Gemischem (1906).

22. LAAR, J. J. van K. Akad. Wet. Proc., 7, 517 (1904).

23. LECAT, L. International Critical Tables, Vol. III, 319 (1933).

24. LELAND, Jr., T. W., McKETTA, Jr., J. J., and KOBE, K. A. IEC, 47, 1265 (1955).

25. NEVENS, T. D. Ph.D. Dissertation, The Ohio State University (1950).

26. OLDS, R. H., SAGE, B. H., and LACEY, W. N. IEC, 34, 1223 (1942).

27. REAMER, H. H., OLDS, R. H., SAGE, B. H., and LACEY, W. N. IEC, 36, 381 (1944).

28. RICCI, J. E. Heterogeneous Equilibrium, D. Van Nostrand Co., Inc., New York (1951).

29. RICHARDS, T. W., CARVER, E. K., and SCHUMB, W. C. JACS, 41, 2019 (1919).

30. ROOSEBOOM, H. W. Heterogeneous Equilibria, Vol. II, part 2, Friedrich Vieweg and Son (1918).

31. SCHEFFER, F. E. C. K. Akad. Wet. Proc., 16, 404 (1913).

32. SCHEFFER, F. E. C. K. Akad, Wet. Proc., 17, 834 (1914).

33. SCHRAER, E. Z. Physik Chem., 142, 365 (1929).

34. SEIDELL, A. Solubilities of Inorganic and Organic Compounds, Vol. II, 3rd Ed., 368 (1941).

35. TSIKILIS, D. S. Dokalady Akad. Nauk SSSR, 86, 1159 (1952).

36. WAALS, J. D. van der Lehrbuches der Thermodynamik, Leipzig (1927).

37. YOUNG, S. Stoichiometry, Longmans Green and Co., New York (1918).

APPENDIX A

CALIBRATIONS

Pressure Gauge

The bourdon pressure gauge was calibrated against a dead weight gauge tester up to a pressure of 3000 psig at increasing and decreasing increments of 50 psi. The results of the calibration were summarized as a continuous smooth curve in the form of a deviation chart (Figure 13).

Prior to the beginning of each consecutive series of observations the dead weight gauge tester and the pressure gauge were isolated from the remainder of the system and the reference zero deviation established.

Thermocouple

A thermocouple made from 24 gauge iron and constantan wire with fiber glass insulation was standardized against melting ice, condensing water vapor, condensing naphthalene vapor, condensing benzophenone vapor, and condensing mercury vapor using a melting ice reference junction. The results of the standardization are summarized in Table V. The standard chart, Table VI, was prepared from the data of Corruccini (5) by graphical differentiation and integration.

A curve (Figure 14) of the deviation of the true E M F of the thermocouple from the standard chart versus the E M F was prepared in order to facilitate interpolation.

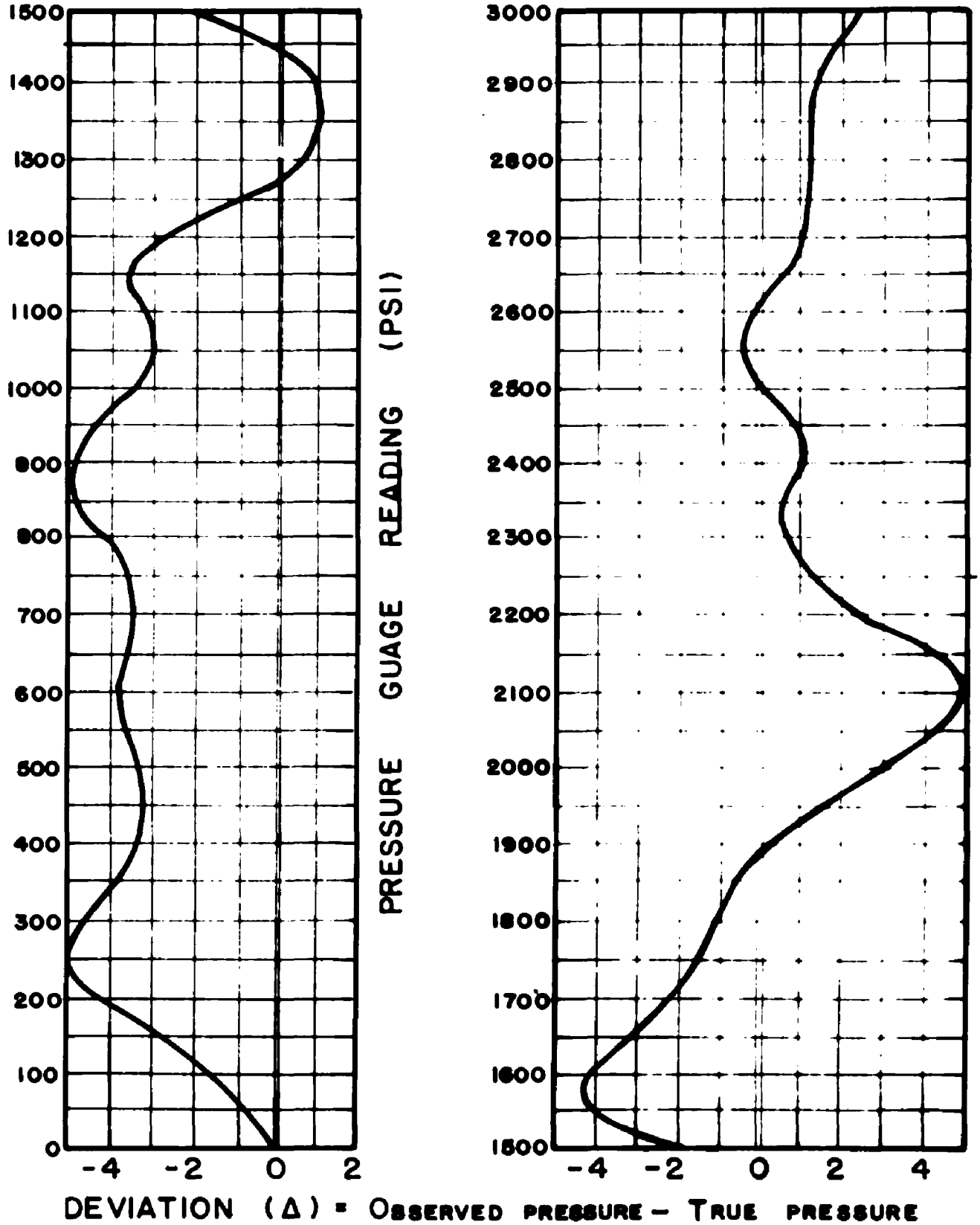

Fig. 13. Pressure Guage Deviation Chart

TABLE V: Thermocouple Standardization Data

Substance	E_o, emf thermo-couple	Baro-metric pressure mm Hg	True temp. °C	E_c emf chart	Devia-tion $E_o - E_c$
Melting ice	-0.0146	743.1	0.00	0.000	-0.0146
Condensing water	5.2420	743.1	99.38	5.2098	+0.0322
Condensing naphthalene	11.7183	741.9	216.87	11.6894	+0.0289
Condensing benzophenone	16.493	735.2	304.28	16.5455	-0.052
Condensing mercury	19.227	736.3	354.94	19.360	-0.033

TABLE VI: Reference Chart for Iron-Constantan Thermocouple

M.V.	0.0	0.1	0.2	0.3	0.4	0.5	0.6	0.7	0.8	0.9
0	2.02	2.02	2.01	2.00	2.00	1.99	1.98	1.98	1.97	1.97
	0.00	2.02	4.04	6.05	8.05	10.05	12.04	14.02	16.00	17.97
1	1.96	1.96	1.95	1.95	1.94	1.94	1.94	1.93	1.93	1.92
	19.94	21.90	23.86	25.81	27.76	29.70	31.64	33.58	35.51	37.44
2	1.92	1.91	1.91	1.91	1.90	1.90	1.90	1.89	1.89	1.89
	39.36	41.28	43.19	45.10	47.01	48.91	50.81	52.71	54.60	56.49
3	1.88	1.88	1.88	1.87	1.87	1.87	1.87	1.86	1.86	1.86
	58.38	60.26	62.14	64.02	65.89	67.76	69.63	71.50	73.36	75.22
4	1.85	1.85	1.85	1.85	1.85	1.84	1.84	1.84	1.84	1.84
	77.08	78.93	80.79	82.63	84.48	86.33	88.17	90.01	91.85	93.69
5	1.84	1.83	1.83	1.83	1.83	1.83	1.83	1.83	1.83	1.82
	95.53	97.37	99.20	101.03	102.86	104.69	106.52	108.35	110.18	112.01
6	1.82	1.82	1.82	1.82	1.82	1.82	1.82	1.82	1.82	1.82
	113.83	115.65	117.47	119.29	121.11	122.93	124.75	126.57	128.39	130.21
7	1.82	1.82	1.82	1.81	1.81	1.81	1.81	1.81	1.81	1.81
	132.03	133.85	135.67	137.49	139.30	141.11	142.92	144.73	146.54	148.35
8	1.81									
	150.16	151.97	153.78	155.59	157.40	159.21	161.02	162.83	164.64	166.45
9	1.81									
	168.26	170.07	171.88	173.69	175.31	177.31	179.12	180.93	182.74	184.55

TABLE VI (continued)

M.V.	0.0	0.1	0.2	0.3	0.4	0.5	0.6	0.7	0.8	0.9
10	1.81 186.36	188.17	189.98	191.79	193.60	195.41	197.22	199.03	200.84	202.65
11	1.80 204.46	206.26	208.06	209.86	211.66	213.46	215.26	217.06	218.86	220.66
12	1.80 222.46	224.26	226.06	227.86	229.66	231.46	233.26	235.06	236.86	238.66
13	1.80 240.46	242.26	244.06	245.86	247.66	249.46	251.26	253.06	254.86	256.66
14	1.80 258.46	260.26	262.06	263.86	265.66	267.46	269.26	271.06	272.86	274.66
15	1.80 276.46	278.26	280.06	281.86	283.66	285.46	287.26	289.06	290.86	292.66
16	1.80 294.46	296.26	298.06	299.86	301.66	303.46	305.26	307.06	308.86	310.66
17	1.80 312.46	314.26	316.06	317.86	319.66	321.46	323.26	325.06	326.86	328.66
18	1.80 330.46	332.26	334.06	335.86	337.66	339.46	341.26	343.06	344.86	346.66
19	1.80 348.46	350.26	352.06	353.86	355.66	357.46	359.26	361.06	362.86	364.66

TABLE VI (continued)

M.V.	0.0	0.1	0.2	0.3	0.4	0.5	0.6	0.7	0.8	0.9
20	1.79									
	366.46	368.25	370.04	371.83	373.62	375.41	377.20	378.99	380.78	382.57
21	1.79									
	384.36	386.15	387.94	389.73	391.52	393.31	395.10	396.89	398.68	400.47
22	1.79									
	402.26									

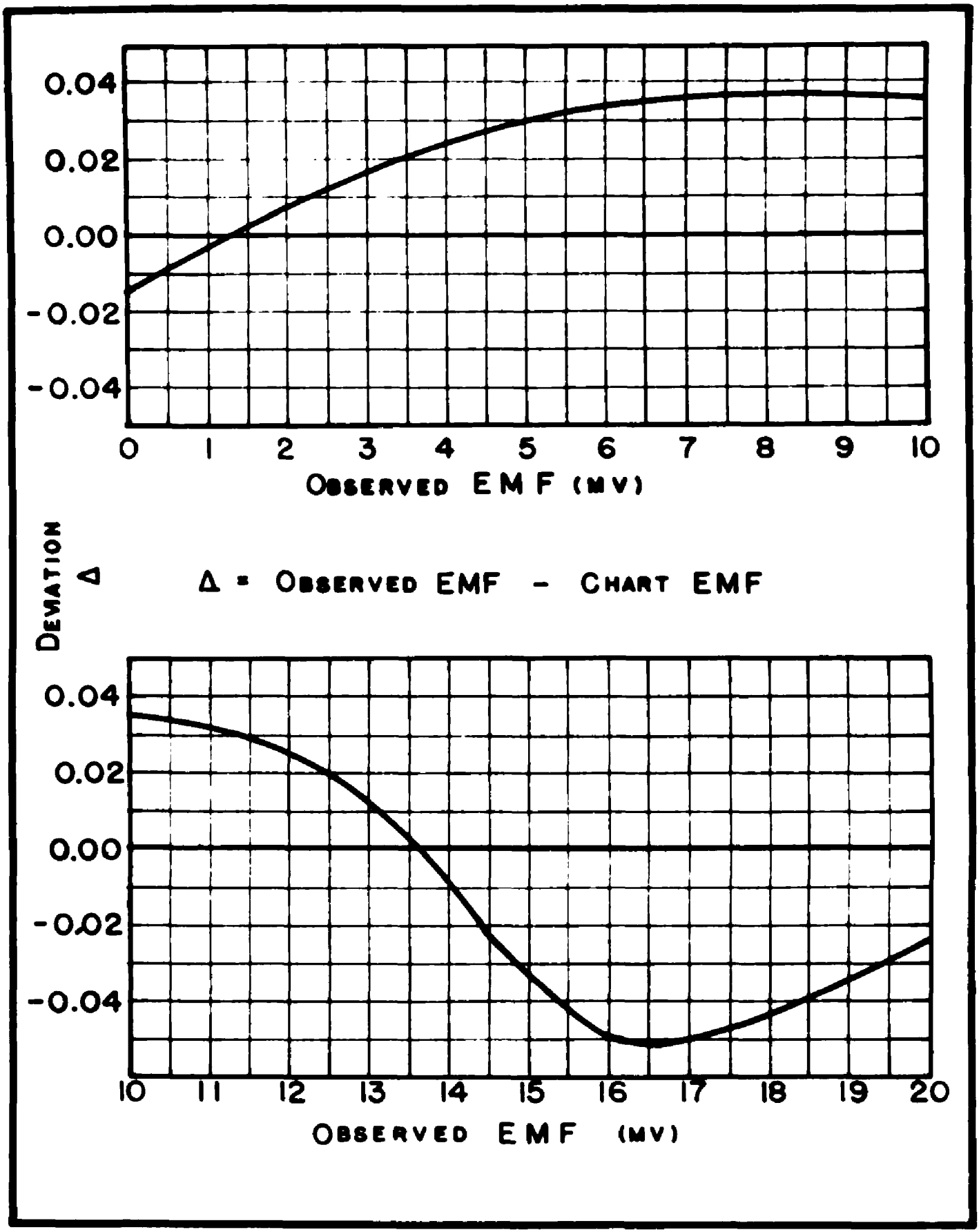

Fig. 14. Thermocouple Deviation Chart

Sample Measuring Tube

The precision-bore capillary tube used for measuring the quantity of each component in a sample mixture was calibrated to determine its volume as a function of its length from the tip. Measurements were made of the length and temperature of known masses of mercury in the tube and of the height of the mercury meniscus. To the calculated volume of mercury was added a volume compliment of the mercury meniscus based on the assumption that the meniscus was a segment of a sphere.

For convenience in subsequent use these data were reduced to the form of a linear equation by application of the method of least squares with the following result:

$$V = 0.00782\ L + 0.00007$$

where: V is the volume in cc
L is the tube length in cm

The total volume of the sampling capillary plus the attached closed stopcock was 16.75 cc.

For samples numbered 1 through 4 a capillary tube calibrated by Donham (7) to have the following volume-length relation was used:

$$V = 0.0003209\ L + 0.00010$$

where: V is the volume in cc
L is the tube length in mm

The total volume of the assembly was 13.41 cc.

APPENDIX B

SAMPLING

Determination of sample composition

From the measurements made on the individual components the actual composition of the sample was calculated in a manner shown in Table VII for sample numbered 15. The individual items in the table have the following significance:

1. The temperature of the water bath surrounding the sample measuring capillary tube.
2. The vapor pressure of the individual components at the temperature of the bath.
3.& 4. Cathetometer readings of the length of the liquid.
5. The difference of items 3 and 4.
6. The calculated volume of liquid.
7. The calculated number of gram-mols of component contained in the remainder of the volume of the measuring tube assembly at its saturated vapor pressure and temperature assuming an ideal gas.
8. The mass of the vapor.
9. The mass of the liquid.
10. The total mass of each component.
11. The total mass of the sample.
12. The composition of the sample.

TABLE VII: Sample Calculation of Mixture Composition

Sample No. 15

1.	Bath temperature °C	9	12
2.	Vapor pressure mm Hg	43	10
3.	Meniscus level (cm)	62.900	65.065
4.	Tube tip (cm)	61.695	61.665
5.	Liquid length (cm)	1.205	3.400
6.	Liquid volume (cc)	0.00949	0.02665
7.	Mol vapor (gm mol)	4.13×10^{-5}	0.948×10^{-5}
8.	Weight vapor (gm)	0.00322	0.00017
9.	Weight liquid (gm)	0.00834	0.02665
10.	Total weight component (gm)	0.01156	0.02682
11.	Sample weight (gm)	0.03838	
12.	Composition weight per cent	30.1	69.9

APPENDIX C

EXPERIMENTAL RAW DATA

Data on phase behavior

The data on phase behavior for samples of fixed composition are presented in Table VIII as they were originally observed and corrected for the known deviations of the measuring instruments.

Extraneous data

During the course of the experiment a series of measurements were made which were construed at the time as representing phase change. Ultimately these measurements were found to be points of equality of refractive index of the two liquid phases. These data are given in Table IX.

TABLE VIII: Experimental Data

Data on Sample No. 1

Composition: 94.7 wt% benzene, 5.3 wt% water — 80.5 mol% benzene, 19.5 mol% water

Observation	Temp. °C	Pressure psia
85	202.4	462
86	205.4	490
87	210.6	539
84	213.5	567
83	223.5	673
91	231.5	763
92	232.0	768
93	232.9	775
94	233.5	782
82	233.7	786
95	234.2	789
96	235.0	796
97	235.6	805
98	236.6	815
99	237.6	822
88	238.6	832
100	238.5	832
101	239.3	841
44	239.6	849
102	240.2	851
103	231.0	861
104	241.9	867
105	242.8	877
81	243.6	882
106	243.6	885
107	244.4	893
108	245.1	901
109	246.0	911
110	246.7	918
111	247.5	925
80	250.8	958
90	255.9	1012
46	256.0	1028
58	256.9	1031
89	257.5	1028
48	264.9	1114
59	266.0	1123
60	267.6	1136
50	267.9	1137
61	269.2	1146
65	270.9	1147
62	270.8	1151
63	271.2	1144
64	271.3	1142
66	271.6	1134
67	271.9	1129
78	272.2	1127
79(c)	272.3	1127
68	272.2	1126
69	272.3	1122
70	272.4	1120
71	272.6	1118
73	272.7	1112
74	272.8	1110
77	273.0	1100
76	273.0	1078
75	272.8	1063
72	272.7	1055
57	272.9	1034
56	272.5	1019
55	271.6	996
52	269.6	958
51	267.9	920
49	264.9	877

Data on Sample No. 2

Composition: 90.6 wt% benzene, 9.4 wt% water — 69.0 mol% benz., 31.0 mol% water

112	207.7	513
113	211.9	553
114	217.5	612
115	222.8	671
116	227.5	725
117	231.7	753
118	235.7	828
119	239.3	879
120	242.9	921

TABLE VIII (continued)

Data on Sample No. 2 (con't)
Composition:
90.6 wt% benzene
9.4 wt% water
69.0 mol% benzene
31.0 mol% water

Observation	Temp. °C	Pressure psia
121	246.2	961
126	248.2	995
123	252.0	1031
124	254.6	1062
129	256.1	1092
125	257.3	1094
128	260.0	1139
127	265.0	1194
130	266.4	1207
131	267.9	1217
132	268.4	1220
133	268.8	1219
134	269.1	1218
135	269.4	1216
136	269.6	1210
137(c)	269.7	1207
138	269.9	1203
141	270.3	1197
142	270.4	1193
145	270.8	1183
146	270.9	1169
144	270.8	1153
143	270.6	1141
139	270.3	1130
140	270.3	1129
147	269.2	1089
148	268.7	1069
149	267.9	1061
150	266.1	1027
158	266.4	1025
151	264.8	994
157	262.4	948
153	258.9	904
156	255.8	849
154	254.5	830
155	247.9	742

Data on Sample No. 3
Composition:
88.2 wt% benzene
11.8 wt% water
63.3 mol% benzene
36.7 mol% water

Observation	Temp. °C	Pressure psia
159	255.6	1091
160	258.9	1133
161	261.3	1164
162	263.8	1190
163	265.9	1216
164	268.4	1217
165	269.4	1230
166	269.5	1227
167(c)	269.6	1224
168	269.8	1220
170	270.1	1214
171	270.2	1210
174	270.4	1200
173	270.4	1181
172	270.3	1175
169	270.1	1162
176	270.0	1157
177	268.7	1112
178	267.2	1072
179	265.4	1037
180	261.8	961
181	257.2	901

Data on Sample No. 4
Composition:
80.6 wt% benzene
19.4 wt% water
48.9 mol% benzene
51.1 mol% water

182	250.7	1041
183	254.6	1105
184	257.6	1156
185	260.0	1202
189	261.6	1239

TABLE VIII (continued)

Data on Sample No. 4(con't)
Composition:
80.6 wt% benzene
19.4 wt% water
48.9 mol% benzene
51.1 mol% water

Observation	Temp. °C	Pressure psia
186	262.8	1250
190	264.9	1295
191	265.8	1314
192	266.7	1326
193	267.0	1329
194	267.3	1334
195	267.5	1338
196(c)	267.8	1334
197	267.6	1327
198	267.5	1322
199	267.4	1315
200	266.7	1299
201	265.1	1284
202	264.3	1241
203	260.9	1168
208	257.9	1113
204	254.4	1056
207	249.6	976
206	244.2	895
205	238.8	813

Data on Sample No. 5
Composition:
74.3 wt% benzene
25.7 wt% water
40.1 mol% benzene
59.9 mol% water

Observation	Temp. °C	Pressure psia
211	228.5	729
210	246.5	978
212	257.5	1162
209	258.2	1165
213	261.0	1219
217	262.4	1251
214	265.0	1289
218	264.4	1293
219	265.7	1331
215	267.3	1333
216	267.8	1341
220	267.2	1346
221	268.0	1353
222	268.1	1356
224	267.6	1361
225	267.6	1348
226	266.9	1328
227	265.5	1302
228	263.3	1263
229	260.3	1204
230	256.1	1131
231	249.2	1007

Date on Sample No. 6
Composition:
63.9 wt% benzene
36.1 wt% water
29.0 mol% benzene
71.0 mol% water

Observation	Temp. °C	Pressure psia
255	243.7	937
256	248.0	1008
236	263.7	1280
237(c)	268.1	1361
251	268.6	1361
292	291.8	2665
296	291.5	2526
297	293.2	2203
284	296.8	2002
283	298.0	1991
299	298.3	2021
282	299.4	1991
281	299.6	1956
249	298.4	1939
248	298.0	1911
280	298.7	1909
279	297.7	1887
247	296.0	1832
246	293.8	1750
278	293.1	1711
245	291.6	1678
244	289.3	1616
277	287.9	1586

TABLE VIII (continued)

Data on Sample No. 6(con't)
Composition:
63.9 wt% benzene
36.1 wt% water
29.0 mol% benzene
71.0 mol% water

Observation	Temp. °C	Pressure psia
243	287.0	1558
24?	284.7	1494
270	283.0	1463
241	281.9	1431
240	279.2	1372
239	275.8	1315
238	272.8	1250
235	271.8	1233
234	268.1	1155
233	264.2	1082
232	259.7	1019

Data on Sample No. 7
Composition:
49.1 wt% benzene
50.9 wt% water
18.2 mol% benzene
81.8 mol% water

Observation	Temp. °C	Pressure psia
301	265.9	1322
302(c)	268.4	1364
341	296.7	2874
342	299.0	2860
367	296.7	2843
344	297.7	2794
368	297.5	2783
369	298.1	2671
343	299.0	2519
345	299.6	2471
328	300.4	2450
346	300.6	2406
347	301.9	2357
348	303.4	2319
349	304.2	2309
327	304.4	2304
350	304.8	2305
352	305.5	2304
326	305.7	2295
351	305.7	2302
353	306.4	2301
354	307.2	2305
325	307.4	2310
355	307.9	2312
356	309.1	2316
370	310.0	2326
357	310.2	2328
371	310.9	2335
314	311.4	2333
372	311.8	2347
373	312.9	2356
374	313.8	2369
316	314.2	2371
360	314.5	2383
375	315.2	2383
376	315.7	2396
361	316.2	2406
377	316.9	2408
362	317.9	2421
378	318.1	2421
363	319.0	2436
379	319.3	2434
364	320.2	2440
380	320.8	2438
324	321.0	2406
322	321.7	2380
323	321.0	2317
320	319.9	2225
317	317.1	2114
315	314.2	2020
310	313.5	2000
313	311.4	1937
309	310.4	1900
312	308.0	1838
308	307.3	1805
307	303.9	1718
306	300.2	1619
305	296.5	1517
304	291.6	1413
303	286.0	1307

TABLE VIII (continued)

Data on Sample No. 8
Composition:
71.2 wt% benzene
29.9 wt% water
35.4 mol% benzene
64.6 mol% water

Observation	Temp. °C	Pressure psia
396	252.6	1093
403	255.8	1144
398	258.5	1198
405	260.8	1237
400	263.1	1288
409	268.0	1366
414	277.0	2275
412	278.2	2143
418	277.8	2117
417	279.8	1997
416	281.7	1797
415	282.2	1679
395	283.1	1664
393	281.8	1620
392	280.0	1569
391	277.7	1514
390	275.2	1456
389	272.9	1406
388	269.8	1352
387	266.8	1289
386	264.1	1239
385	261.2	1180
384	257.4	1111
383	253.8	1051
382	250.0	973

Data on Sample No. 9
Composition:
35.1 wt% benzene
64.9 wt% water
11.1 wt% benzene
88.9 mol% water

Observation	Temp. °C	Pressure psia
421	259.4	1197
420	263.4	1275
419(c)	268.4	1364
455	297.7	2728
454	298.9	2541
453	300.5	2426
452	301.9	2361
451	303.0	2335
456	303.5	2326
450	304.2	2314
449	305.4	2305
457	305.2	2304
458	306.7	2302
459	308.4	2309
447	309.1	2318
460	310.2	2328
461	311.7	2349
446	315.5	2402
445	321.4	2489
444	325.1	2546
443	327.8	2586
433	329.3	2604
435	331.5	2640
437	333.3	2669
439	335.3	2684
442	336.2	2674
441	336.2	2626
438	335.3	2545
436	333.3	2411
434	331.5	2347
432	329.1	2290
431	326.9	2207
430	324.6	2112
429	322.1	2033
428	319.5	1957
427	317.0	1862
426	314.1	1800
425	311.2	1741
424	308.1	1639
423	301.7	1494

Data on Sample No. 10
Composition:
22.0 wt% benzene
78.0 wt% water
6.1 mol% benzene
93.9 mol% water

462	257.7	1177
463	260.7	1236
464	264.9	1304
465(c)	267.7	1364

TABLE VIII (continued)

Data on Sample No. 10(con't)
Composition:
22.0 wt% benzene
78.0 wt% water
6.1 mol% benzene
93.9 mol% water

Observation	Temp. °C	Pressure psia
468	293.7	2513
467	295.0	2337
466	296.6	2246
469	298.0	2187
470	300.0	2125
475	300.9	2123
471	301.7	2120
474	302.1	2121
473	302.7	2119
472	303.2	2126
476	303.9	2132
477	306.1	2150
478	308.3	2171
479	310.8	2207
480	313.3	2242
483	316.6	2304
484	319.5	2352
487	322.8	2406
488	325.6	2467
491	329.1	2530
492	333.2	2615
495	337.1	2698
496	341.2	2777
499	345.6	2855
503	346.3	2868
502	347.4	2881
501	349.7	2914
506	350.9	2917
500	349.7	2771
498	345.7	2593
497	341.2	2425
494	337.1	2300
493	333.2	2152
490	329.1	2084
489	325.6	1932
486	322.8	1850
485	319.5	1760
482	316.6	1682
481	313.2	1569

Data on Sample No. 11
Composition:
6.0 wt% benzene
94.0 wt% water
1.5 mol% benzene
98.5 mol% water

Observation	Temp. °C	Pressure psia
507	246.2	985
508	248.0	1024
509	252.5	1081
510	256.6	1151
511	260.1	1216
512	266.4	1244
513	269.2	1274
514	275.6	1329
515	281.5	1374
516	289.3	1467
517	296.2	1564
518	304.1	1665
519	314.2	1824
520	322.0	1989
521	329.3	2137
522	335.9	2293
523	341.6	2435
524	346.5	2567
525	349.1	2685
526	355.7	2826
528	357.4	2875

Data on Sample No. 12
Composition:
11.7 wt% benzene
88.3 wt% water
3.0 mol% benzene
97.0 mol% water

529	254.7	1126
530	258.1	1184
531	261.3	1247
532	264.4	1303
533	266.5	1340
534	267.6	1362
535(c)	268.0	1365
537	283.4	1915
546	284.6	1819

TABLE VIII (continued)

Data on Sample No. 12(con't)
Composition:
11.7 wt% benzene
88.3 wt% water
3.0 mol% benzene
97.0 mol% water

Observation	Temp. °C	Pressure psia
545	285.8	1779
544	287.5	1763
538	288.4	1765
543	289.6	1767
542	290.7	1784
539	293.0	1799
540	297.3	1836
541	301.4	1890
547	305.5	1941
548	310.2	2020
549	314.8	2094
550	320.3	2184
551	325.3	2289
553	329.9	2388
554	334.1	2479
555	334.1	2060
552	329.9	1932

Data on Sample No. 13
Composition:
40.6 wt% benzene
59.4 wt% water

Observation	Temp. °C	Pressure psia
556	260.9	1218
557	262.9	1254
558	265.4	1303
559	267.8	1350
560(c)	268.5	1366
578	329.5	2561
577	327.3	2548
576	324.9	2516
575	322.4	2483
574	319.9	2441
573	317.0	2402
572	314.2	2360
579	312.3	2342
580	313.0	2352
588	312.0	2338
571	311.1	2323
587	310.0	2321
570	308.4	2299
586	308.2	2302
569	307.2	2294
585	306.5	2298
568	305.8	2295
584	305.0	2299
567	304.4	2304
583	303.9	2306
566	303.3	2319
565	302.3	2340
582	301.8	2343
564	301.3	2373
561	300.9	2400
562	299.5	2464
563	298.6	2552
581	299.2	2557

Data on Sample No. 14
Composition:
38.2 wt% benzene
61.8 wt% water

592	268.6	1364
610	320.3	2467
609	317.8	2424
608	315.2	2382
607	313.7	2361
606	312.3	2338
605	310.2	2315
604	309.3	2311
603	308.5	2302
602	307.9	2299
601	307.8	2297
600	307.0	2296
599	306.3	2296
598	305.7	2297
597	305.0	2303
596	304.0	2306
595	303.7	2312
594	302.7	2336
593	300.8	2401

TABLE VIII (continued)

Data on Sample No. 15
Composition:
30.1 wt% benzene
69.9 wt% water

Observation	Temp. °C	Pressure psia
618	336.6	2713
619(c)	336.1	2711
617	336.0	2708
616	335.5	2701
615	333.4	2671
614	331.8	2643
613	331.4	2632
612	329.1	2604
611	328.2	2585

TABLE IX: The Pressure-Temperature Relations at Points of Equal Refractive Index for Two Liquid Phases

Sample No. 6

Observation	Temp. °C	Pressure psia
254	252.5	1149
257	255.4	1251
258	257.2	1314
259	258.8	1389
263	259.6	1402
253	259.7	1418
260	261.5	1474
261	264.0	1513
262	265.4	1640
252	268.6	1725
264	271.4	1864
288	271.9	1887
265	273.1	1933
266	276.4	2045
267	279.3	2143
289	281.2	2312
293	283.2	2351
268	284.5	2356
294	285.3	2422
269	287.0	2424
295	285.4	2460
290	287.2	2476
287	288.2	2511
291	289.7	2571

Sample No. 7

330	250.6	1132
331	269.8	1857
332	273.1	1958
333	276.4	2076
334	278.7	2158
335	282.5	2334
336	285.1	2408
337	287.6	2518
338	290.2	2665
339	292.3	2748
340	294.4	2859

Sample No. 8

Observation	Temp. °C	Pressure psia
404	255.8	1307
397	258.6	1402
406	260.8	1495
399	262.9	1585
407	264.6	1650
401	267.7	1772
408	269.0	1795
410	271.0	1916
411	275.4	2048

APPENDIX D

The following equipment is standard and commercially available:

Pressure gauge: 16-inch dial, 750 graduations, range zero to 5000 psi. Heise Bourdon Tube Laboratories, Newtown, Connecticut.

Oil booster pump: 10-ton ram, 1.6 cubic inch per stroke, Porto-power pump. Blackhawk Manufacturing Company, Milwaukee, Wisconsin.

Oil compressor piston: Range zero to 15,000 psi, hydraulic pressure generator, Cat. No. 46-9315. American Instrument Company, Incorporated, Silver Spring, Maryland.

Dead weight gauge tester: Modified from Star Brass Manufacturing Company, Boston, Massachusetts.

The following equipment was constructed in the laboratories:

Condensing vapor jacket: The jacket was made completely out of Pyrex glass with the main working section surrounded by a silvered vacuum jacket.

Mercury level indicator and mercury compressor piston: These items of equipment are shown by Hoekelman (12) in detailed drawings.

AUTOBIOGRAPHY

I, Charles J. Rebert, was born in Ann Arbor, Michigan, December 27, 1918. I received my secondary school education in the public schools of Detroit, Michigan. My undergraduate training was obtained at The University of Detroit, from which I received the degree Bachelor of Chemical Engineering in 1943. From the University of Michigan I received the degree Master of Science in Engineering in 1948. In October, 1950, I received an appointment as Instructor at The Ohio State University, where I specialized in the Department of Chemical Engineering. I held this position for five years while completing the requirements for the degree Doctor of Philosphy.